(12) SDAC-TR-79-8

LEVEL II

AD A093169

EVALUATION OF THE NATIONAL SEISMIC STATION

I.T. Noponen, E.B. McCoy, and H.S. Sproules
Seismic Data Analysis Center
Teledyne Geotech, 314 Montgomery Street, Alexandria Virginia 22314

12 December 1979

Sponsored by

The Defense Advanced Research Projects Agency (DARPA)

DARPA Order No. 2551

Monitored By

AFTAC/VSC

312 Montgomery Street, Alexandria, Virginia 22314

Unclassified

SECURITY CLASSIFICATION OF THIS PAGE (When Data Entered)

REPORT DOCUMENTATION PAGE

READ INSTRUCTIONS BEFORE COMPLETING FORM

1. REPORT NUMBER: (14) SDAC-TR-79-8	2. GOVT ACCESSION NO.: AD-A093	3. RECIPIENT'S CATALOG NUMBER: 769
4. TITLE (and Subtitle): (6) EVALUATION OF THE NATIONAL SEISMIC STATION.		5. TYPE OF REPORT & PERIOD COVERED: (9) Technical rept.
		6. PERFORMING ORG. REPORT NUMBER
7. AUTHOR(s): (10) I. T. Noponen, E. B. McCoy, H. S. Sproules		8. CONTRACT OR GRANT NUMBER(s): (15) F08606-79-C-0007, ARPA Order-2551
9. PERFORMING ORGANIZATION NAME AND ADDRESS: Teledyne Geotech, 314 Montgomery Street, Alexandria, Virginia 22314 (12) 54		10. PROGRAM ELEMENT, PROJECT, TASK AREA & WORK UNIT NUMBERS: VT/9709
11. CONTROLLING OFFICE NAME AND ADDRESS: Defense Advanced Research Projects Agency, Nuclear Monitoring Research Office, 1400 Wilson Blvd. Arlington, Virginia 22209 (11)		12. REPORT DATE: 12 December 1979
		13. NUMBER OF PAGES: 51
14. MONITORING AGENCY NAME & ADDRESS (if different from Controlling Office): VELA Seismological Center, 312 Montgomery Street, Alexandria, Virginia 22314		15. SECURITY CLASS. (of this report): Unclassified
		15a. DECLASSIFICATION/DOWNGRADING SCHEDULE

16. DISTRIBUTION STATEMENT (of this Report)

APPROVED FOR PUBLIC RELEASE; DISTRIBUTION UNLIMITED.

17. DISTRIBUTION STATEMENT (of the abstract entered in Block 20, if different from Report)

18. SUPPLEMENTARY NOTES

19. KEY WORDS (Continue on reverse side if necessary and identify by block number)

National Seismic Station, Dynamic Range, System Noise, Nonlinearity, Signal-to-Noise Ratio, P Waves, L_g Waves, Tele-Communication, Data Acquisition, Regional Earthquakes, SDCS

20. ABSTRACT (Continue on reverse side if necessary and identify by block number)

The resolution in A/D conversion when recording waveforms of night-time (low) noise on four different NSS channels at CPO is 0.3 to 1% of the RMS noise power. Clipping of the middle period (MP) and long period (LP) channels in A/D conversion was observed in the case of an M_S = 7.6 shock at a distance 22°, and signal amplitudes up to 30% of the clipping level were observed on the short-period channel when recording nondestructive local shocks (up to 1°). In one such case a probably spurious waveform was observed on the vertical MP

DD FORM 1473, 1 JAN 73 — EDITION OF 1 NOV 65 IS OBSOLETE

Unclassified

SECURITY CLASSIFICATION OF THIS PAGE (When Data Entered)

408258 slt

and LP channels, suggesting non-linear behavior of the analog system at large voltages. A similar phenomenon has been observed at an SRO station.

Coherencies computed between the SDCS and NSS channels, i.e., between independent sets of instruments both located at CPO, indicate that when recording night-time (low) noise, the earth-motion/system-noise ratio is good (> 4) up to 60% of the folding frequency for the LP and MP channels. The short-period channel of the Model I NSS seems to have extraneous noise above 4-5 Hz, and it is able to record earth noise down to ~ 0.15 Hz. The vertical HF channel seems to have system noise at frequencies around 2 Hz which, in some cases, obscures the earth noise.

SNR computations suggest that regional phases (P and L_g) can be easily detected above 5 Hz; L_g waves from an NTS shot at a distance of 22° had their maximum SNR at a period of 4 seconds. P-waves from teleseismic events generally had SNR maxima at 1 Hz, poor SNR above 5 Hz, and a deep minimum around periods of 4-5 seconds. However, a large (m_b = 6.4) event had its P-wave SNR maximum at a period of 10 seconds; probably this was caused by a highly attenuating shock-to-receiver path.

Also discussed in this evaluation is the data link format and communications preprocessing. There were several problem areas, primarily with time code procedures, in the NSS site design.

EVALUATION OF THE NATIONAL SEISMIC STATION

SEISMIC DATA ANALYSIS CENTER REPORT NO.: SDAC-TR-79-8

AFTAC Project Authorization No.:	VELA-T/9709/B/PMP
Project Title:	Seismic Data Analysis Center
ARPA Order No.:	2551
Name of Contractor:	TELEDYNE GEOTECH
Contract No.:	F08606-79-C-0007
Date of Contract:	01 October 1979
Amount of Contract:	$1,493,393
Contract Expiration Date:	30 September 1980
Project Manager:	Robert R. Blandford (703) 836-3882

P. O. Box 334, Alexandria, Virginia 22313

APPROVED FOR PUBLIC RELEASE; DISTRIBUTION UNLIMITED.

ABSTRACT

The resolution in A/D conversion when recording waveforms of night-time (low) noise on four different NSS channels at CPO is 0.3 to 1% of the RMS noise power. Clipping of the middle period (MP) and long period (LP) channels in A/D conversion was observed in the case of an M sub s M_s = 7.6 shock at a distance 22 deg, and signal amplitudes up to 30% of the clipping level were observed on the short-period channel when recording nondestructive local shocks (up to 1 deg). In one such case a probably spurious waveform was observed on the vertical MP and LP channels, suggesting non-linear behavior of the analog system at large voltages. A similar phenomenon has been observed at an SRO station.

Coherencies computed between the SDCS and NSS channels, i.e., between independent sets of instruments both located at CPO, indicate that when recording night-time (low) noise, the earth-motion/system-noise ratio is good (> 4) up to 60% of the folding frequency for the LP and MP channels. The short-period channel of the Model I NSS seems to have extraneous noise above 4-5 Hz, and it is able to record earth noise down to about ~ 0.15 Hz. The vertical HF channel seems to have system noise at frequencies around 2 Hz which, in some cases, obscures the earth noise.

SNR computations suggest that regional phases (P and L_g) can be easily detected above 5 Hz; L_g waves from an NTS shot at a distance of 22 deg had their maximum SNR at a period of 4 seconds. P-waves from teleseismic events generally had SNR maxima at 1 Hz, poor SNR above 5 Hz, and a deep minimum around periods of 4-5 seconds. However, a large (m sub b m_b = 6.4) event had its P-wave SNR maximum at a period of 10 seconds; probably this was caused by a highly attenuating shock-to-receiver path.

Also discussed in this evaluation is the data link format and communications preprocessing. There were several problem areas, primarily with time code procedures, in the NSS site design.

TABLE OF CONTENTS

LIST OF FIGURES

LIST OF FIGURES (Continued)

1. INTRODUCTION

The National Seismic Station (NSS) is intended to provide seismic data to support the verification of a Comprehensive Test Ban Treaty. It is intended to provide both regional and teleseismic measurements over a wide frequency range and a large dynamic range. The system provides three-component seismic measurement from a period of 50 seconds to a frequency of 10 Hz. The Model I data used in this study also contains a high-frequency channel recording the vertical component with a sampling rate of 60 samples per second. Gain ranging and analog-to-digital conversion are provided for each of the bands.

The NSS used in this study is situated in the Cumberland Plateau Observatory (CPO). The seismometers and associated electronics are deployed in a cased borehole at the depth of 100m. The seismometers of a Special Data Collection System (SDCS) station are situated at 100m in a second borehole at a distance of 10m from the first. This gave an opportunity to compare records from the two recording systems. Such a comparison was one of the goals of this investigation. The other goals were to evaluate the technique of using gain-ranging in the analog-to-digital conversion, in terms of precision and clipping level; and to study the signal-to-noise ratios of local, regional, and teleseismic events in the broad frequency range provided by the four channels of the NSS system.

The seismological results obtained from an on-line observatory depend not only on the characteristics of the sensing instrument and A/D system, but also on the telecommunication links, the data acquisition computer and processing systems, and their reliability. In implementing the on-line data acquisition, several weak areas were uncovered, and we intend to summarize this experience.

2. THE NSS AND SDCS STATIONS

The design goals of the NSS were (Durham, 1979) to have digitized seismic data with adequate signal level to allow recovery of earth noise from a frequency band as narrow as a half octave (i.e. to have the sensitivity limited by external noise rather than system noise), to preserve teleseismic capability, to have minimal phase and amplitude distortions in the data band, to output true ground motion (velocity) records and to provide unattended remote station operation.

Since seismic signals have a very large dynamic range which is further increased by the large changes of the spectral level across the wide frequency band which is monitored, gain ranging and spectral filtering are used in NSS to increase the limited dynamic range achieved in the analog-to-digital conversion (ADC) process. The seismometers are assumed to satisfy the design goals related to frequency range, dynamic range and sensitivity. The ADC uses 14 bits which provides an 84 dB dynamic range, and the gain ranging provides additional 42 dB. The resolution given by the first figure is 1 part in 16383 peak-to-peak.

The response of the four NSS channels is shown in Figure 1, and the responses of the SDCS short-period (SP) and long-period (LP) systems are shown in Figure 2. The essential novelties in NSS, in addition to the gain-ranging system, are the middle-period (MP) and high-frequency (HF) channels. The MP channel gives a large part of the wide-band coverage (0.02-1.0 Hz). As a result of the attempt to minimize phase and amplitude distortion, the microseismic spectral peak near 0.2 Hz is not discriminated against and it dominates the record. The MP channels provide a continuous spectrum over frequencies where the conventional LP and SP combination has a deep null. In combination with SP, MP provides coverage of the entire 0.02 to 5 Hz spectrum. The HF channels extends the recoverable frequency range from about 5 Hz, which is the upper limit for a SP channel sampled 20 times per second, to about 15 Hz.

Durham, H. B. (1979). NSS seismic data system, design goals and rationale; manuscript (Sandia Laboratory), February 14.

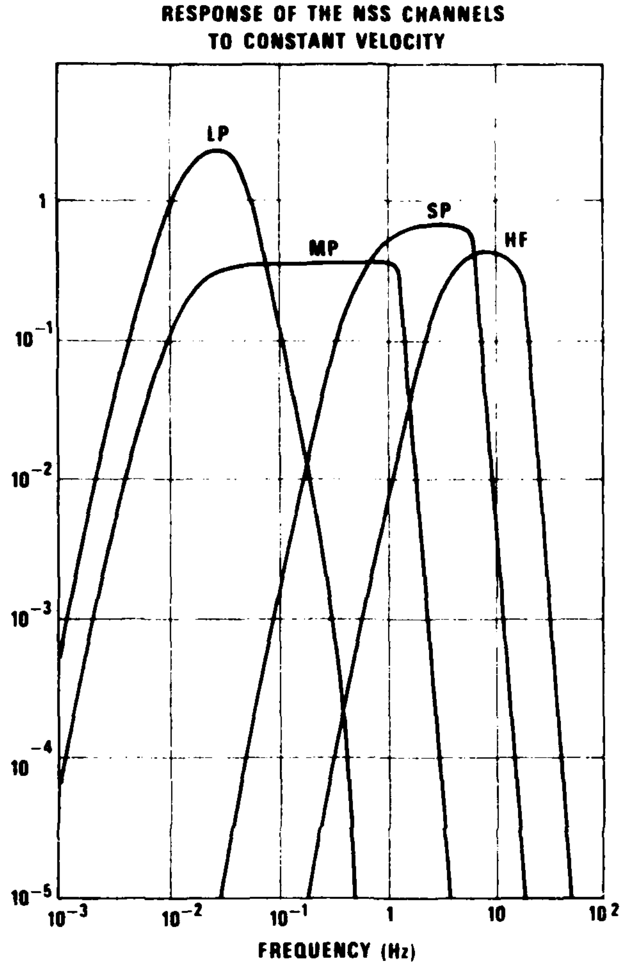

Figure 1. The velocity responses of the four NSS recording channels.

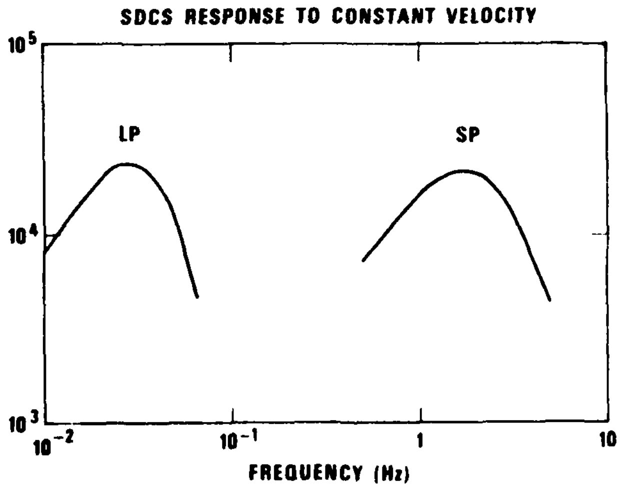

Figure 2. The velocity responses of the SDCS long-period and short-period seismographs.

The gain of the LP channel is higher than that of the MP channel around a period of 20 seconds. Its strong low-pass filtering makes it insensitive to the main microseismic peak at 5 s period. It thus gives a higher resolution and provides a record from which weak surface waves can be detected without further filtering. Also, the SP channel has been planned to provide the capability to detect weak teleseismic P waves without further filtering, in the short-period "noise window."

The NSS seismographs are a KS-36000, which provides the SP, MP and LP 3-component recordings, and a S-600, which provides the HF vertical recording and acts as a back-up seismometer to which the other vertical channels can be switched in case of failure of the KS-36000 unit.

3. QUANTIZATION AND CLIPPING IN THE NSS A/D CONVERSION

In the gain-ranging system, the gain can be varied in four steps (gain factors 1, 8, 32, and 128). When recording background noise the gain setting has its highest value. We computed the RMS noise values measured in quantization units, from the (night-time) noise samples shown in Figure 3 (sample 27). The HF and SP channels had RMS values 101 and 132, respectively, and the MP and LP channels had somewhat higher values 315 and 270 q.u., respectively. These RMS values are higher than those of the SDCS system, and consequently produce smaller digitization error.

If we assume the quantization (rounding) error made in A/D conversion to be random, its standard deviation is 0.29 quantization units (Otnes and Enochson, 1978), or from 0.1 to 0.3% of the RMS noise amplitude recorded on the NSS channels, i.e. insignificant when the recorded waveform is considered.

The gain-ranging system makes clipping a scarce phenomenon on NSS records. It was observed, however, on the LP and MP channels from the $M_s = 7.6$ earthquake in Guerrero, Mexico, at a distance of 21° from NSS (Figure 4). The zero-to-peak amplitude in quantum units is 1,048,576 at the clipping level as expected from a dynamic range of 120 dB (126 dB for peak-to-peak amplitude). When the ADC system is clipping, the analog system is presenting voltage of over ten volts to the A-D converter.

The SP channels of NSS do not clip at the time of arrival of the P-wave from the Mexican earthquake. The LP channels clip during the whole event, from P to surface waves. The MP channels clip during the S wave and in the maximum phase of the surface waves.

Figure 5 shows the maximum amplitudes of a number of events and of a noise sample, read from the different channels and plotted using the quantization level as unit. It can be seen that several of the events have amplitudes over 10% of the clipping level and that teleseismic signals have their largest quantization levels in the long-period channels, while the regional shocks have them in the short-period channels.

Otnes, R. K. and L. Enochson (1978). Applied Times Series Analysis, Volume I., Basic Techniques, John Wiley and Sons, New York.

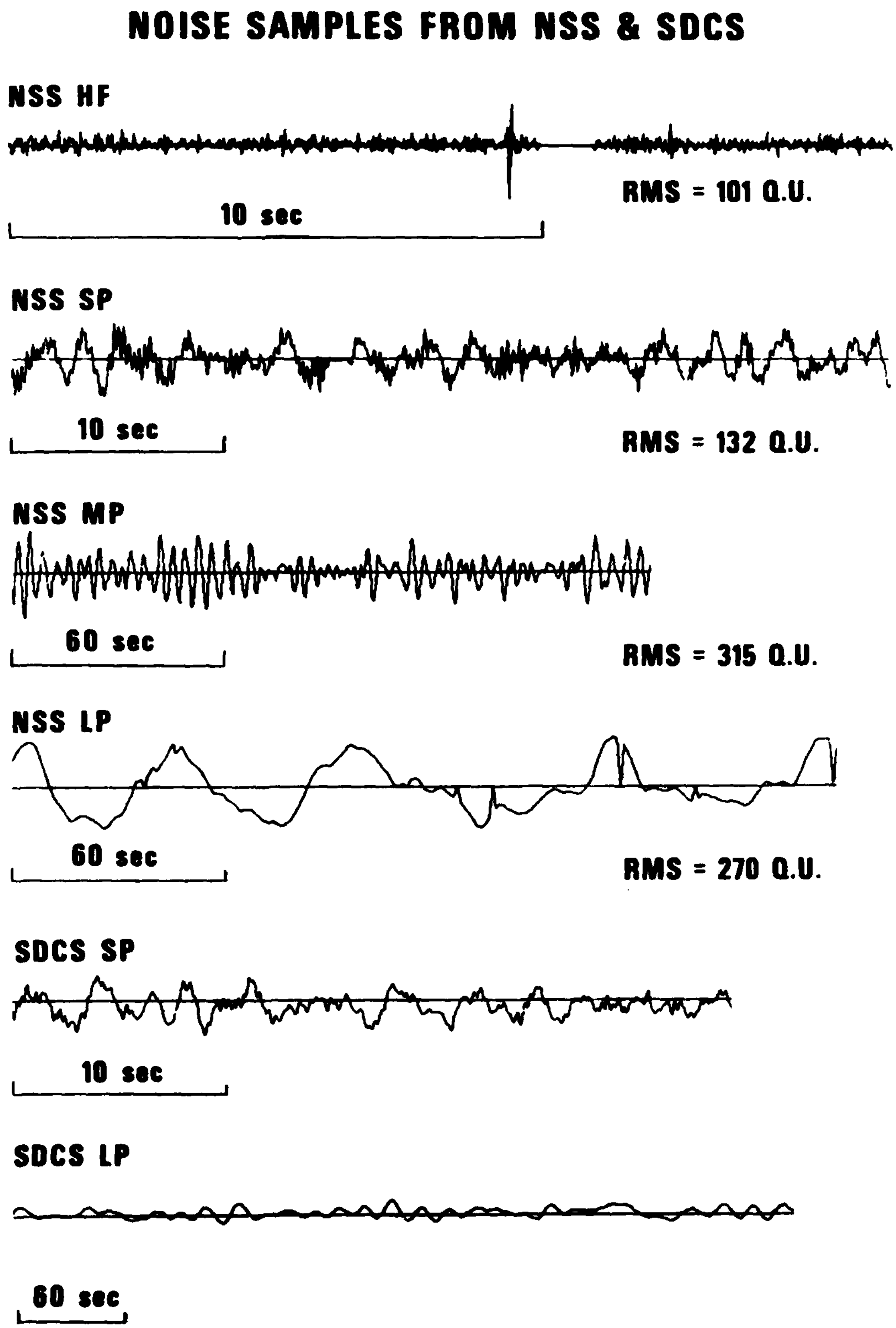

Figure 3. Records of noise from the four NSS recording channels and from the SDCS SP and LP seismographs. Part of the noise sample No. 27 (ref. App. 1) is shown.

14 MAR 1979 (MEXICAN QUAKE) CPO

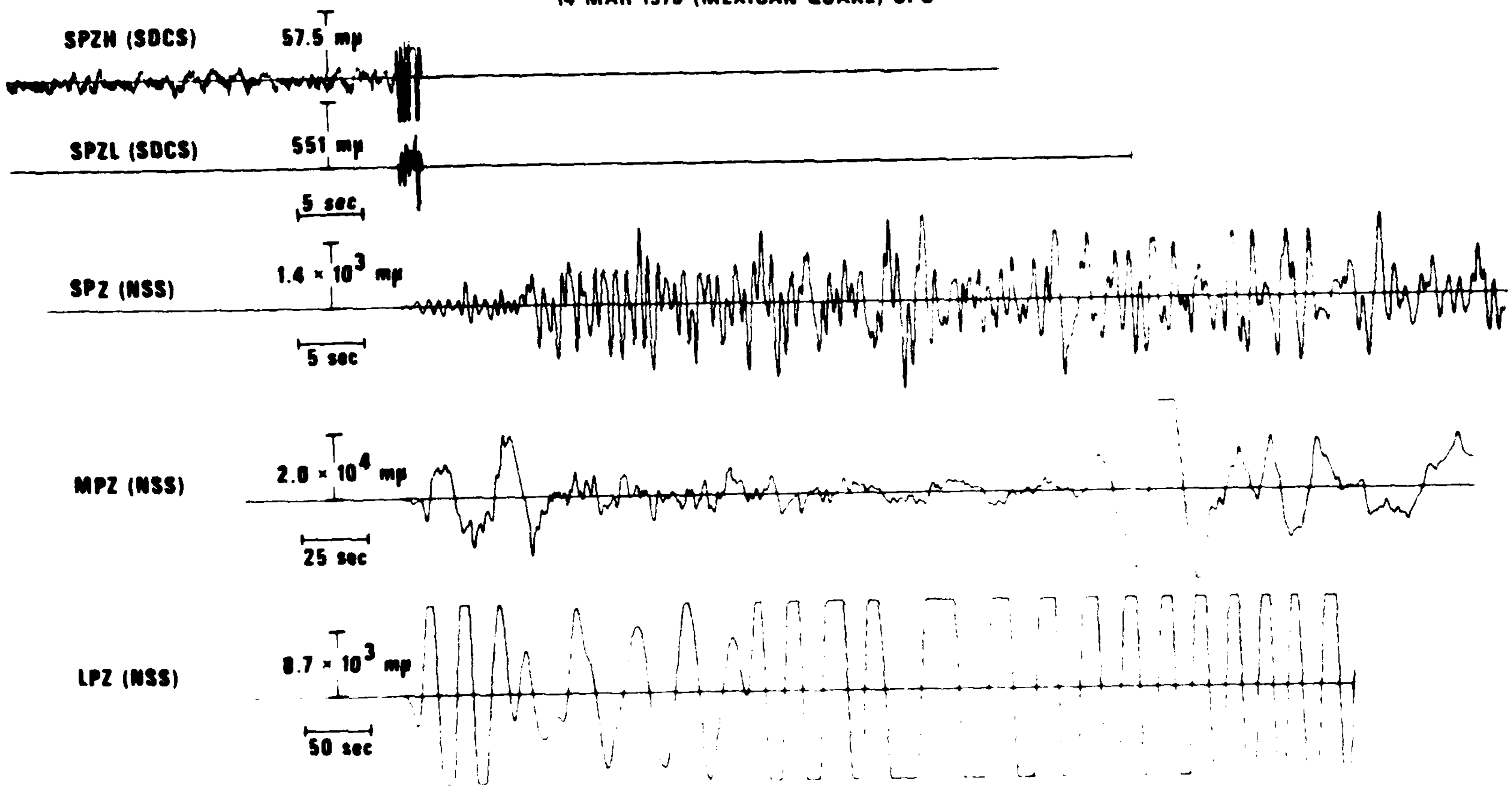

Figure 4. Records of the March 14, 1979 Mexican earthquake (M_s = 7.6) recorded at CPO. The records from the top are the high-gain and low-gain vertical SP records from SDCS (severe clipping), the vertical SP record from NSS (no clipping, the MP vertical record from NSS (some clipping) and the LP vertical record from NSS (strong clipping).

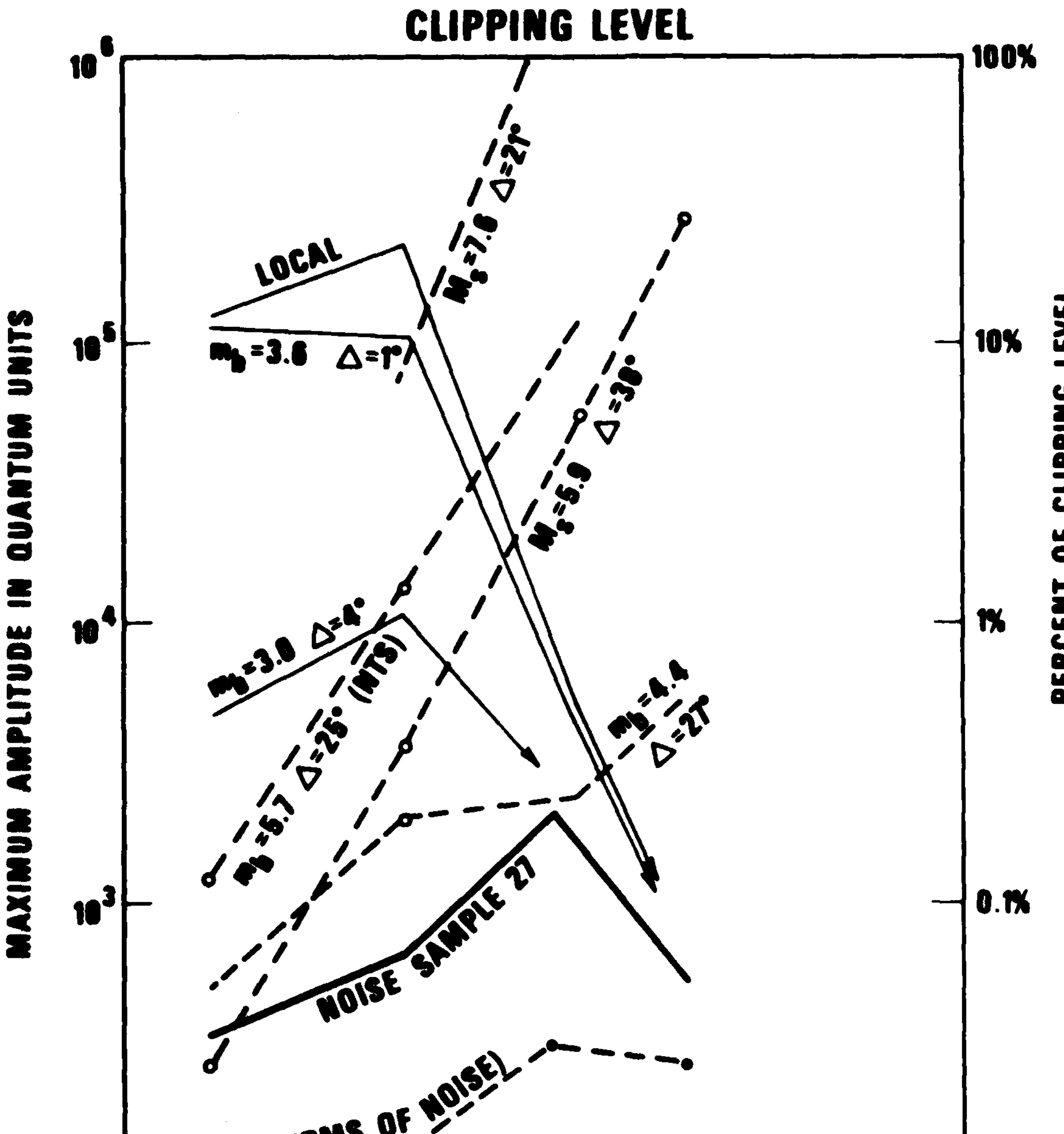

Figure 5. Maximum amplitudes (in quantum units) of data recorded through the four different NSS channels; from regional and local events (thin lines), from teleseismic events (heavy broken lines) and from a noise sample (No. 27 of App. 1, heavy line). The RMS value of the noise sample is also shown. The scale is given both in quantum units and as per cent of the clipping level. The teleseismic maximum amplitudes at LP and MP were associated with the arrival of surface waves.

By scaling the event magnitudes up by the clipping level/maximum amplitude ratio we roughly estimated how much larger each event should have been to cause clipping in the various NSS channels. For teleseismic events, the LP channel is the first to clip. The SP and HF channels may not clip at all from teleseismic events, since for very large magnitudes, say above $M_s = 7.0$, the short-period P wavetrain is lengthened but its amplitudes do not increase much further with magnitude. After scaling up 3 shallow earthquakes at distances 20 to 40 degrees (numbers 9, 10 and 14 in Appendix 1) and assuming the maximum amplitude to fall off with distance at the same rate as the surface wave amplitude (as estimated by von Seggern, 1977) we conclude the clipping limits for LP to be about $M_s = 6.0$ at 20° and $M_s = 7.0$ at 100°. The limits are about one M_s unit higher for the MP channel so that, at the distance 40°, MP clipping would occur for shocks with $M_s > 7.1$. The MP channel acts as a back-up channel for LP, since LP information can be extracted from the MP. The information is summarized in Figure 6. The stated limits are only approximate.

For regional events the SP channel is first to approach clipping. Scaling up four events in the distance range 1 to 5 degrees and assuming the maximum amplitude to decay in eastern U.S. as proportional to the inverse square of distance (Romney et al., 1962), we conclude the m_b magnitude limit required to cause clipping of the SP channels at a distance of 4° to be larger than 5.0, probably larger than 5.5. We can give only the lower estimate for the clipping limit, since with increasing event magnitude energy shifts away from the frequencies spanned by the SP channels so that SP amplitudes increase at a markedly lower rate. The information used is shown in Figure 7.

---

von Seggern, David (1977). Amplitude distance relation for 20-second Rayleigh waves, Bull. Seism. Soc. Am., 67, 405-411.

Romney, C., B. G. Brooks, R. H. Mansfield, D. S. Carder, J. N. Jordan and D. W. Gordon (1962). Travel times and amplitudes of principal body phases recorded from GNOME, Bull. Seism. Soc. Am., 52, 1057-1074.

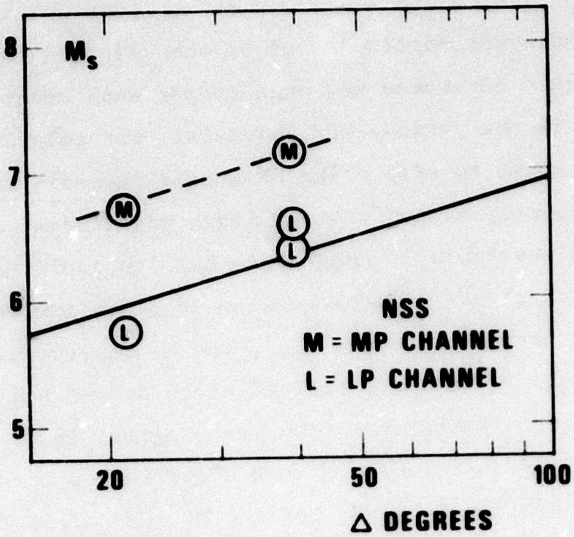

Figure 6. Estimated clipping levels in terms of magnitude M_s as a function of distance for the LP and MP channels. The circles are magnitudes, which have been scaled up from the original event magnitudes according to the ratio of clipping level to the observed maximum level. The continuous line extrapolates the LP data, assuming the LP maximum amplitude to decrease with distance as proportional to $\Delta^{-1.07}$.

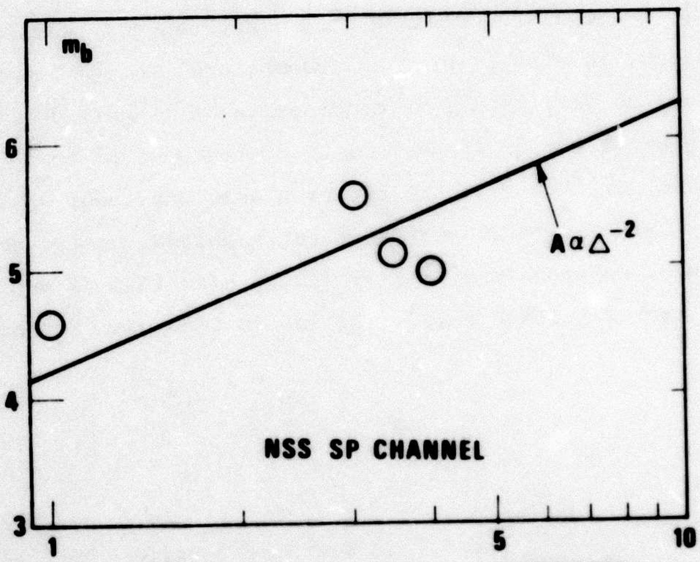

Figure 7. The estimated lower bound of clipping level of the SP channel in terms of magnitude m_b as a function of distance. The circles are magnitudes scaled up from the event magnitudes according to the ratio of clipping level to the observed maximum level. The line extrapolates the data, assuming the maximum amplitude to be proportional to Δ^{-2}. The actual clipping levels may be higher than these because of energy shifting to lower frequencies with increasing magnitude.

The discussion above has been only on the A-D conversion. We also have electrical noise in the system, and we may have nonlinear behavior in the analog system prior to A-D conversion. In the case of earthquake 31 (distance 1.0°) with SP amplitudes 30% of the clipping level, the vertical MP and LP channels show a long-period (about 30 sec) oscillation (see Figure 8). It cannot be seen on the horizontal channel. We suspect it to be a non-linear response to the strong high-frequency excitation of the analog system, because it is unusual for the vertical component of an earth motion to have over 20 times larger amplitudes than the horizontal component, as is the case of the LP signals shown in Figure 8. Clipping was observed in the analog system of the SRO station at Mashad (Goncz and Noponen, 1979), producing spurious pulses on its LP channel when large regional events were recorded.

Goncz, J. and I. Noponen (1979). Relationship between M_s and m_b for small earthquakes in Uzbekistan, USSR, VELA Seismological Center Research Review, 26-27 September.

UN

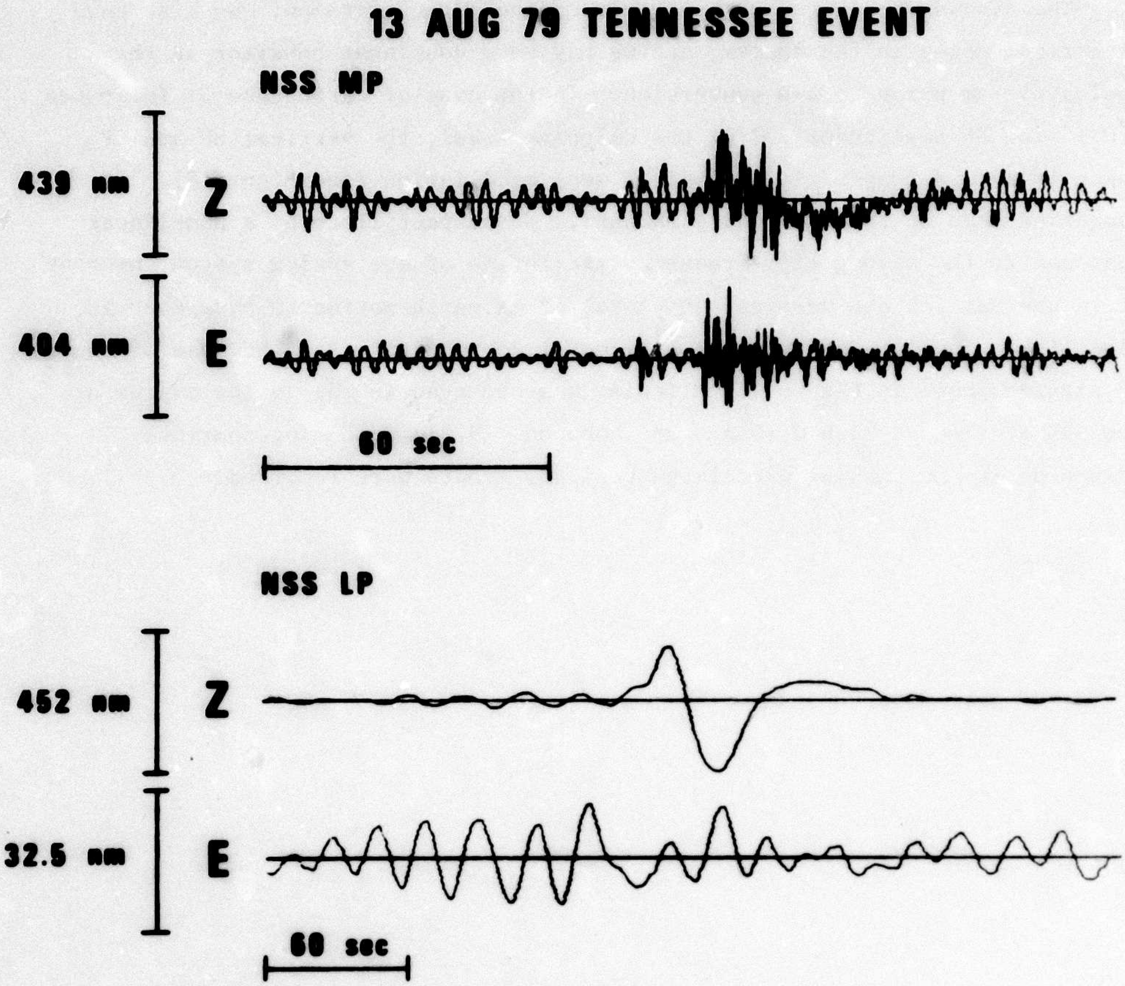

Figure 8. NSS MP (top) and LP (bottom) recordings of an earthquake (Δ = 1.0°, m_b(LG) = 3.6°) showing a spurious-looking long-period oscillation on the vertical channels. We suggest this to be a non-linear response to the large high-frequency earth motion. Vertical channel is marked by Z, east-west component by E. No north-south channel was recorded.

4. SPECTRAL COMPARISON OF SDCS AND NSS RECORDS

Response-corrected noise spectra computed from a noise sample (sample 27) taken at 1:30 a.m. on May 3, 1979 for the various vertical recording channels of the CPO are shown in Figure 9. The agreement between the spectra, where they overlap, is reasonably good considering the stability of the determinations, and that exactly the same time windows could not be used from different channels, due to the different sampling rates. There are disagreements, however, e.g., at the high frequency end of the MP spectral band (marked as END of MP in the figure). This phenomenon is caused by the fact that when the folding frequency is approached (2 Hz for MP, 0.5 Hz for LP) the antialiasing filters cause the system noise to dominate over the signal from the Earth. The strong disagreement between the LP channel of SDCS and the other channels above 0.1 Hz is associated with the notch filter in SDCS at frequency 0.16 Hz. System noise dominates the spectrum in the notch filter rejection band, and when the system (and filter) response is corrected for, this noise forms a peak in the spectrum. All spectra computed for common NSS and SDCS records agreed in the way shown in Figure 9, with less agreement close to the folding frequencies.

Coherences were computed between the vertical NSS and SDCS channels. This allowed us to observe whether, in each narrow frequency band, the same waveform is recorded by the two stations. Whenever coherence is high between the two independent recording systems situated at a distance of 10 m from each other, the earth motion is probably recorded. When coherence is low, system noise in one or both systems is interfering with or covering the signal from the earth. It may well happen that though the earth-motion/system-noise ratio is good in the dominant frequency band, it is poor in some parts of the frequency spectrum. Samples taken at night (low earth-noise conditions) were used.

Coherences between the short-period vertical channels of SDCS and NSS, and between the NSS HF channel and SDCS SP channel are shown in Figure 10. The coherence between SP channels drops sharply at half the folding frequency. In one of the cases, the drop begins already at 4 Hz. Since this is contrary to the NSS design goals, we attempted to find out whether the extraneous noise was in the SDCS or NSS SP system. The ratio of NSS to SDCS

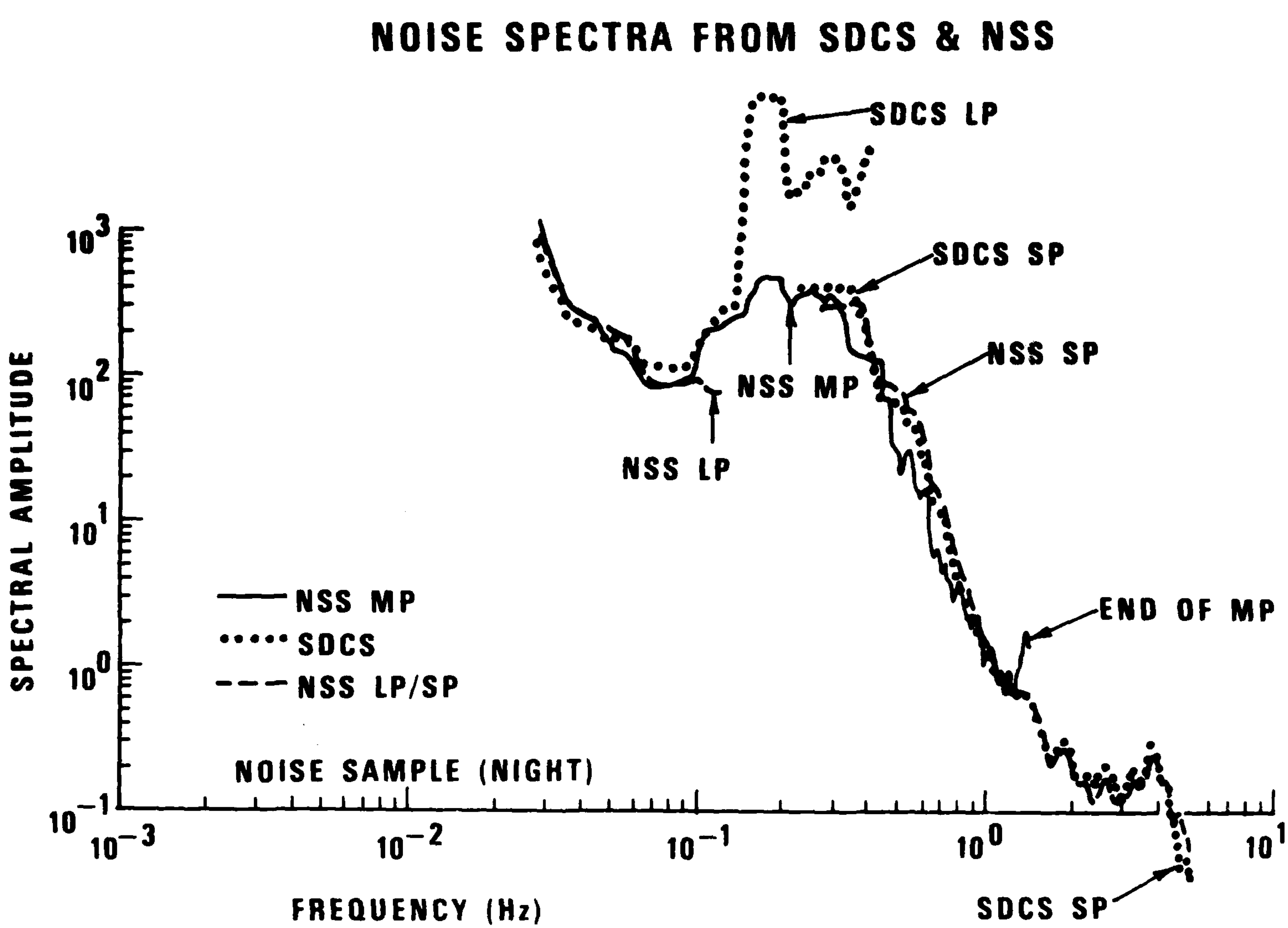

Figure 9. Noise spectra for sample 27 computed from various channels of the SDCS and NSS. The disagreements among the spectra are associated with the ends of the frequency bands (note " END of MP") and the notch filter of the SDCS LP at 0.17 Hz.

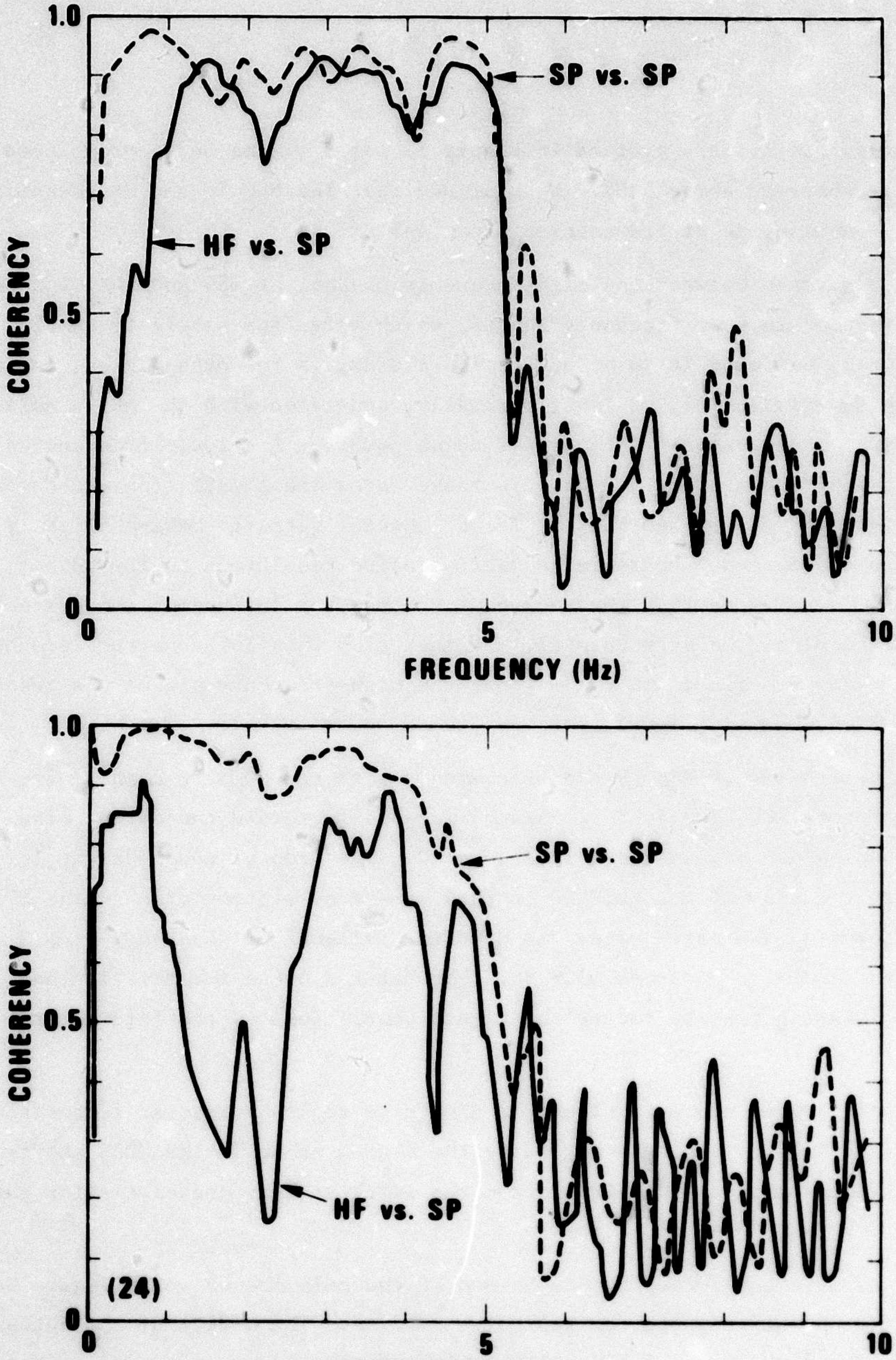

Figure 10. Coherencies computed between NSS SP and SDCS SP traces (broken lines) and the NSS HF and SDCS SP traces (continuous lines). SP to SP coherencies are high (around 0.9) from ~ 0.1 Hz to 40% or 50% of folding frequency. The HF vs SP coherencies are poor in varying frequency ranges below 5 Hz, showing system noise in HF.

short-period spectra are plotted in Figure 11 for 5 traces and a pronounced maximum is observed above 5 Hz. We conclude that the NSS SP and HF channels have extraneous noise at frequencies above 4-5 Hz.

The coherence between the high-frequency channel of NSS and the SDCS SP channel is poor in some frequency ranges, which vary from sample to sample. In two cases, we found it to be poor below 1.0 Hz, in two other cases, around 2 Hz. This variation is, at least partially, connected with the earth noise level, since those samples with higher noise power at the lower frequencies have best coherences below 1.0 Hz. In these cases the signal from the earth motion overrides the system noise. The HF channel seems to behave slightly worse than the intended goals in respect of noise resolution in low-noise conditions. It may be that the choice of seismometer influences the system noise in the high-frequency channel. In the cases with low coherence around 2 Hz (and high coherences in 0.2 - 1 Hz) the high-frequency signal was taken from the KS-36000 seismometer, not from the S-500 as usual.

The coherences of NSS LP and MP channels with the SDCS SP channel are shown in Figure 12. The SDCS SP channel is able to record the earth noise at least up to 4.5 Hz, as shown in Figure 10. The drop of coherence at 1.5 Hz between the NSSP MP and SDCS SP is thus caused by system noise in the MP channel covering the earth noise, as also the fall-off of coherency at 0.3 Hz between the NSS LP and the SDCS SP. The natural cause for this is that the anti-aliasing filters reduce the signal power close to the folding frequency.

The coherences shown in Figure 12 also drop to low values at frequencies smaller than 0.1 Hz. This is caused by the system noise in the SDCS short-period channel covering the signal from the earth at frequencies smaller than 0.1 Hz.

The coherences of the NSS SP, MP and LP channels are shown in Figure 13 against the SDCS LP channel for two noise samples. The effect of the notch filter in the SDCS LP channel is visible in the sharp drop of coherences at 0.17 Hz. In one of the cases the earth noise power seems to be so low compared with the system noise that a broader zone around the notch filter frequency where the SDCS LP response is reduced, shows poor coherences.

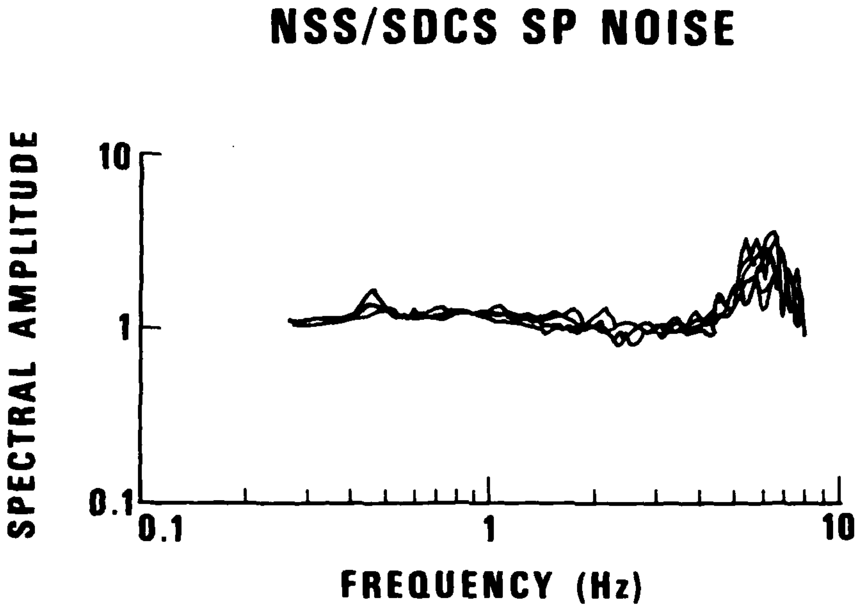

Figure 11. Ratios between response-corrected NSS SP and SDCS SP power spectra computed for five samples of night-time noise. Note the maximum in the ratios above 5 Hz.

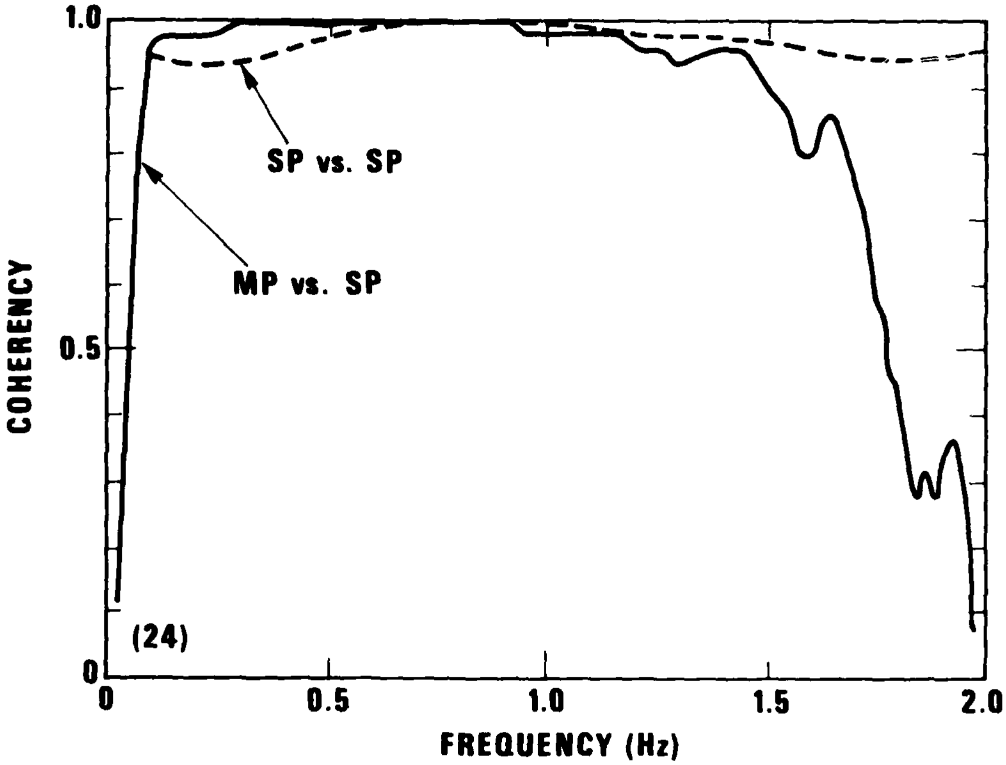

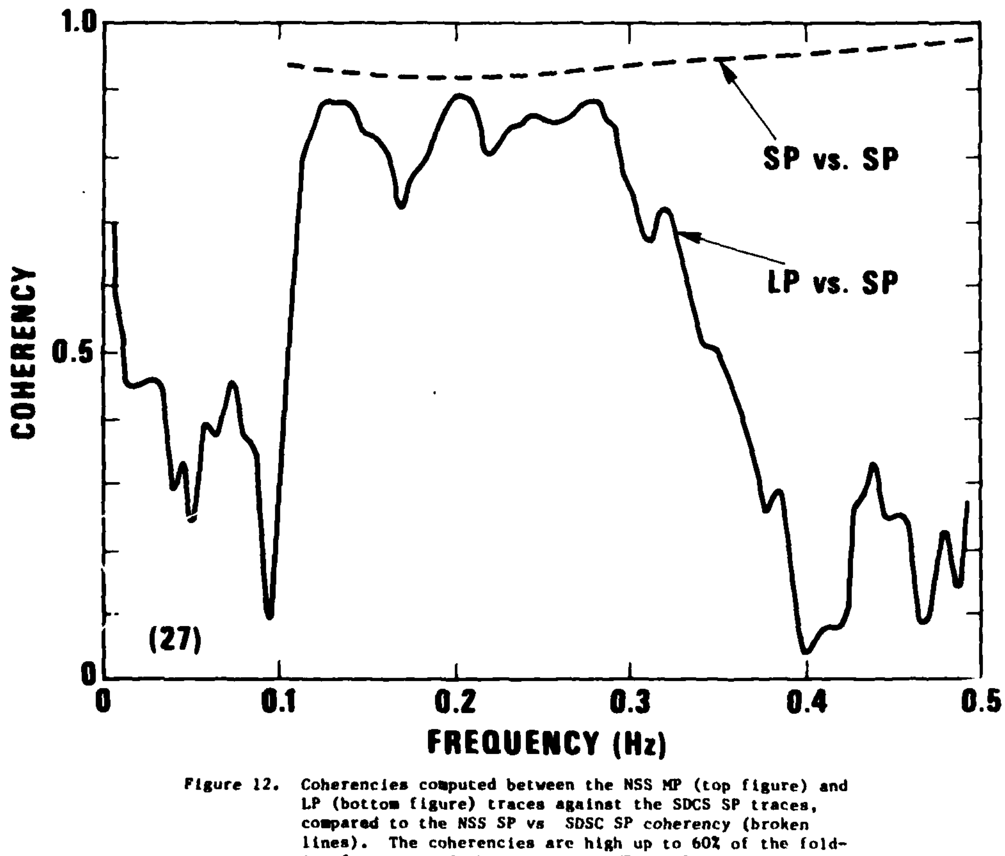

Figure 12. Coherencies computed between the NSS MP (top figure) and LP (bottom figure) traces against the SDCS SP traces, compared to the NSS SP vs SDSC SP coherency (broken lines). The coherencies are high up to 60% of the folding frequency of the respective MP or LP instrument.

The coherences between the NSS and SDCS LP channels are good up to 0.3 Hz, apart from the notch filter. In the noise sample 26 shown in Figure 13 the coherence is poor, however, at frequencies shorter then 0.3 Hz, i.e., at periods longer than 30 s. This is caused by low earth-noise level, since in the other case the LP-to-LP coherency is good down to 0.01 Hz (period 100 seconds).

The coherence between the NSS SP channel and the SDCS LP channel is low at frequencies smaller than 0.15 Hz (period 7 seconds) in the example shown in Figure 13. Since the LP-LP coherency is good to much smaller frequencies, the system noise covers the signal from the earth in the SP channel below 0.15 Hz. This does not mean that strong signals from the Earth could not be recorded at smaller frequencies through the SP channel, but that their detectability is then limited by the system noise.

The coherence between the NSS MP channel and the SDCS LP channels is good, falling slightly below the LP-to-LP coherence at frequencies less than 0.12 Hz. This shows that the earth noise/sytem noise ratio is almost equally good in the NSS MP and LP channels within the LP transmission band, and that the the LP channel can be recovered by suitable filtering of the MP channel.

If the coherence (ζ) is 1.0 between the SDCS and NSS traces, we are able to predict one trace (Y) from the other (X) with perfect accuracy when the system responses are known. We let the transfer function from one trace to another to be H. Introducing system noise our coherence decreases and the prediction H * X becomes inaccurate. The inaccuracy is measured by the ratio between the power on the predicted trace H * X and the residual trace Y - H * X. This is our signal-to-noise ratio. We interpret our coherences in terms of this signal-to-noise ratio, as a function of frequency, which can be derived to be

$$\mathrm{SNR}\left(\frac{\text{signal + noise}}{\text{noise}}\right) = \frac{1}{1 - \zeta^2(f)}$$

which is a quantity ranging from 1 to infinity. Thus a coherence $\zeta = 0.9$ gives an SNR of 5 in predicting one trace from another, 0.71 gives 2.0 and 0.3 gives 1.1. We suggest that coherences above 0.9 mean good signal fidelity, and those above 0.7 mean marginally acceptable.

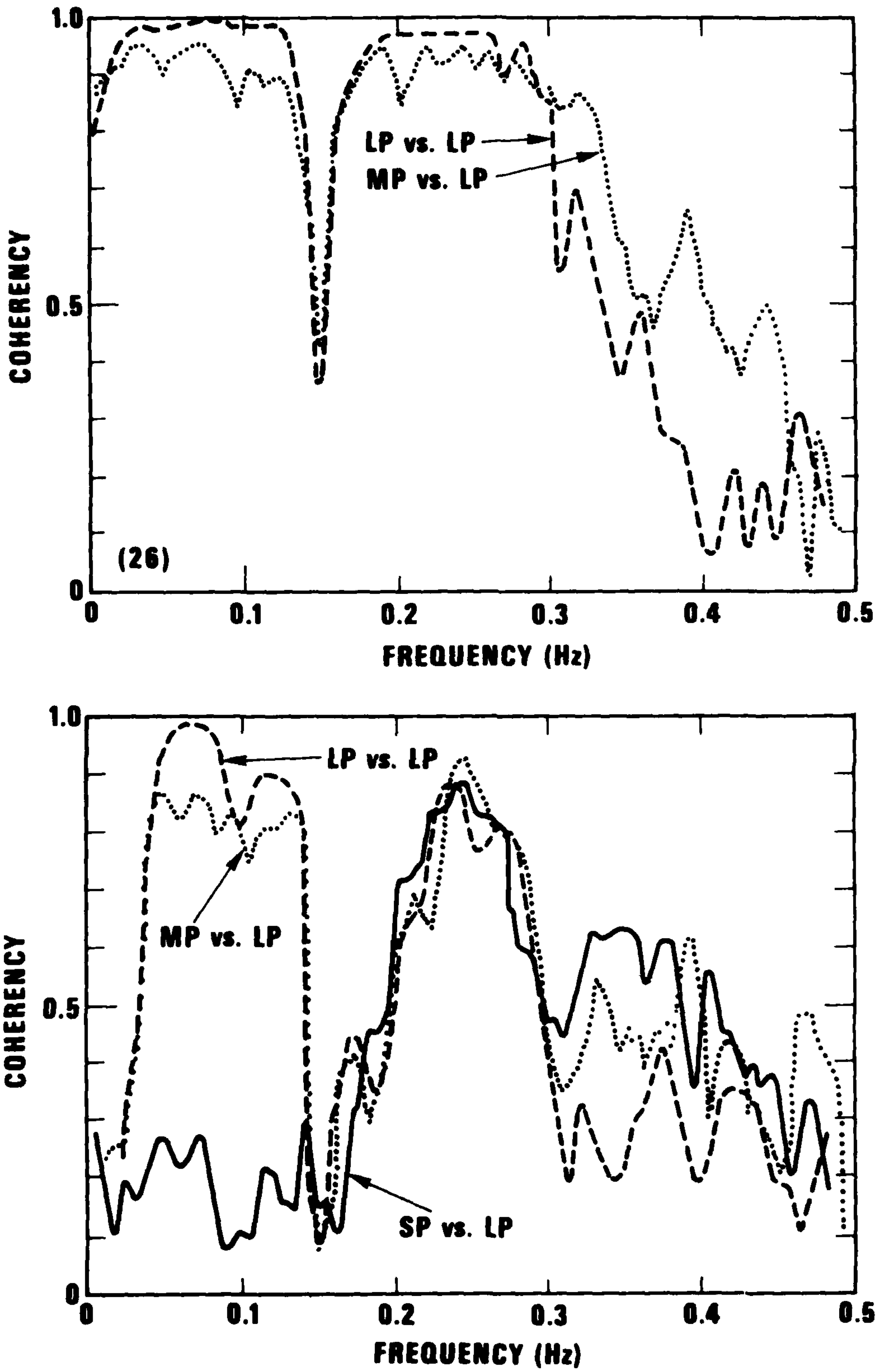

Figure 13. Coherencies between the NSS SP, MP and LP traces against the SDCS LP traces for two night-time noise samples. The SP vs LP coherency is low below 0.15 Hz, showing large system noise at those frequencies.

The examples of results of computations of coherence shown in Figures 10, 12 and 13 span well the range of results which were obtained in computations of coherence from other noise samples. The NSS MP versus SDCS SP coherences in other cases, however, began to fall already at 1.3 Hz as contrasted to the 1.5 Hz shown in Figure 12.

5. EVENT SIGNAL-TO-NOISE RATIOS

We computed spectra for various seismic phases in records from teleseismic and regional events, and for noise samples preceding each event. Signal-to-noise ratios as functions of frequency were formed by dividing the signal spectra by the respective noise spectra. Thus the ratios are signal+noise to noise ratios, but since significant ratios are much larger than one, they approximate well the signal-to-noise ratios. When the ratios oscillated around value 1, we concluded that the true signal-to-noise ratio was small.

SNR's of L_g phases and some other regional phases are plotted in Figure 14. They are combined from NSS HF and SP channels, in some cases also using the MP. When approximately the same time windows were used, the SNR's computed from the various channels agreed, except close to the folding frequencies. There is a distance gap from 5° to 21° due to lack of events in that range.

The events at $\Delta < 5°$ all have significant energy above noise level at frequencies higher than 6 Hz, which is the cut-off frequency of the anti-aliasing filter of the SP system. This applies to other phases as well as to L_g. Thus the high-frequency channel having the 3 dB cut-off frequency 19.5 Hz improves the detectability of regional events and increases the amount of information collected from them. Fitch and Shields (1979) arrived at the same conclusion for a wavepath 5° long in eastern Canada.

The two events at distance 22 and 25 degrees in Figure 14 do not show significant energy above noise at over 6 Hz, as do none of the more distant events studied. The L_g SNR from the NTS shot "PEPATO," at distance 25°, peaks at 0.3 Hz, close to the microseismic spectral peak and in the range of the MP band. The L_g seismograms from "PEPATO," shown in Figure 15, show the largest L_g waves to be in the MP channel. They are typical continental L_g waves with appreciable vertical component. The P-wave signal-to-noise ratios from the "PEPATO" shot and two earthquakes in Mexico are shown

---

Fitch, T. S. and M. W. Shields (1979). Amplitude spectra of crustal phases from a Canadian earthquake, Semiannual Technical Summary (Seismic Discrimination) Lincoln Laboratory, 31 March.

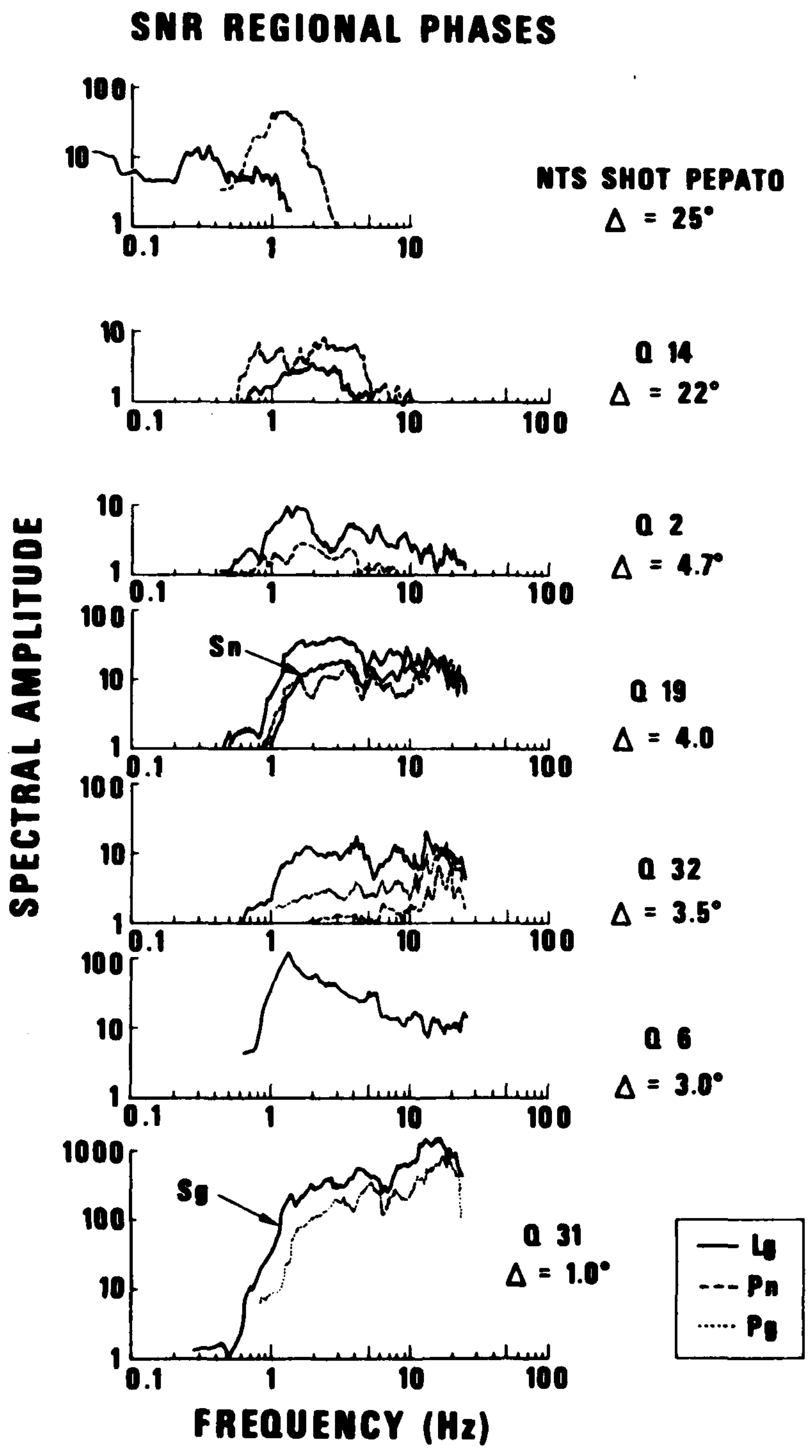

Figure 14. Signal-to-noise ratios (measured by spectral amplitude ratio) of regional seismic phases frou events in the distance range 1° to and 22° to 25°. Quake numbers refer to App. 1.

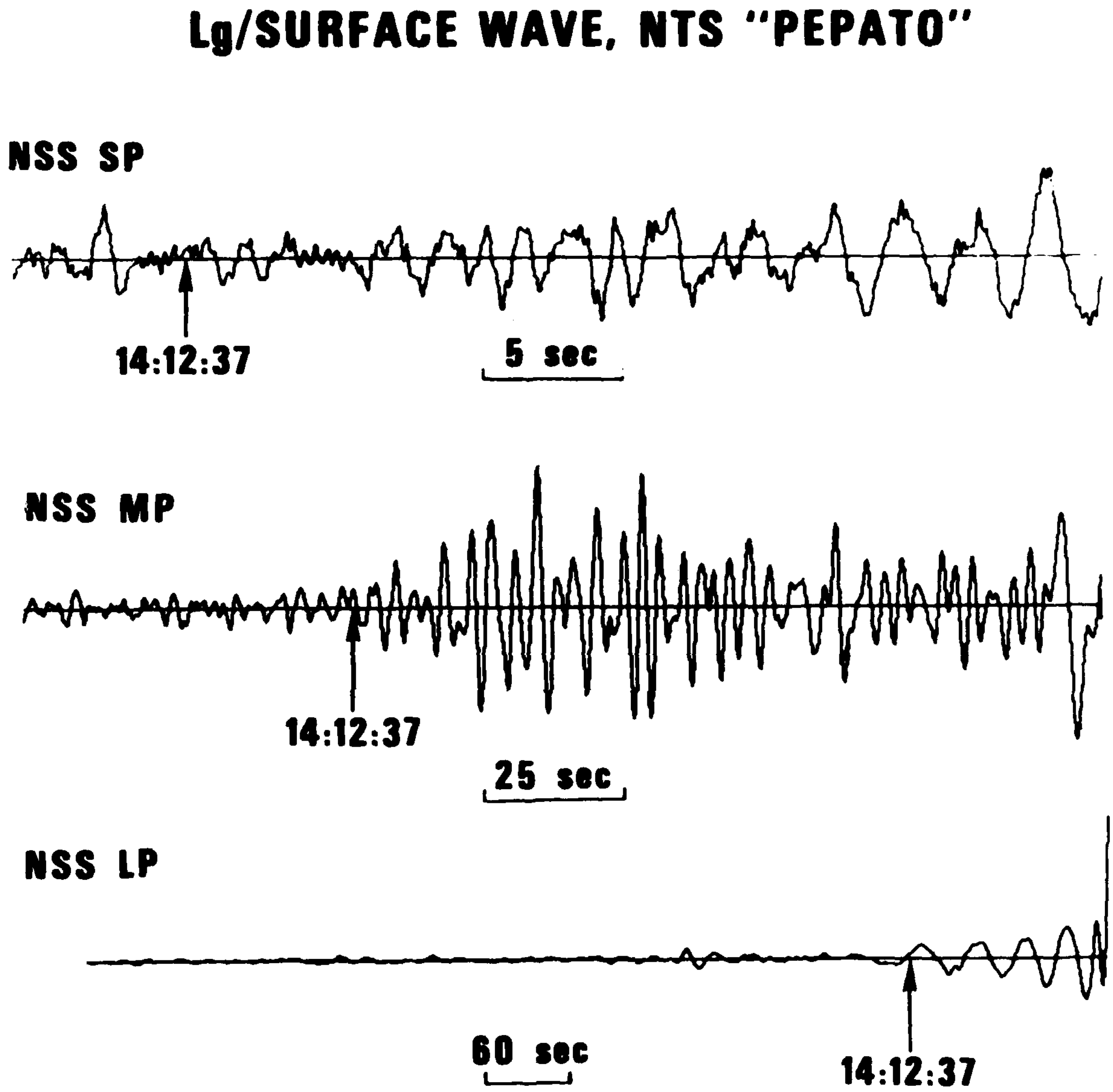

Figure 15. The L_g and surface waves at CPO from the NTS explosion "PEPATO" (m_b = 5.7). Distance to CPO is 25°.

in Figure 16. Distances range from 22 to 25 degrees and no significant energy is seen above the SP high-frequency limit 6 Hz. The P-wave seismograms from the "PEPATO" shot are shown in Figure 17. P-wave signal-to-noise ratios from three earthquakes in S. America are shown in Figure 18. Two of the shocks are shallow, the third ($\Delta = 58°$) has a depth of 101 km. The SNR is seen to fall rapidly above a few Hz, and no significant energy remains above 6 Hz.

Most teleseismic P-waves have their SNR maxima close to 1 Hz and a deep minimum at the frequency of the microseismic noise peak (0.2 Hz). A large shock ($M_s = 5.9$) at the mid-Atlantic Ridge had, however, its P-wave SNR maximum at 0.1 Hz and no minimum at 0.5 Hz, as shown in Figure 19. We suggest this to be caused by large anelastic attenuation of waves under the mid-oceanic ridge suppressing the high-frequency waves. A PKP wave from distance 131° (Molucca Passage source region) has an SNR similar to that of usual P-waves (Figure 19).

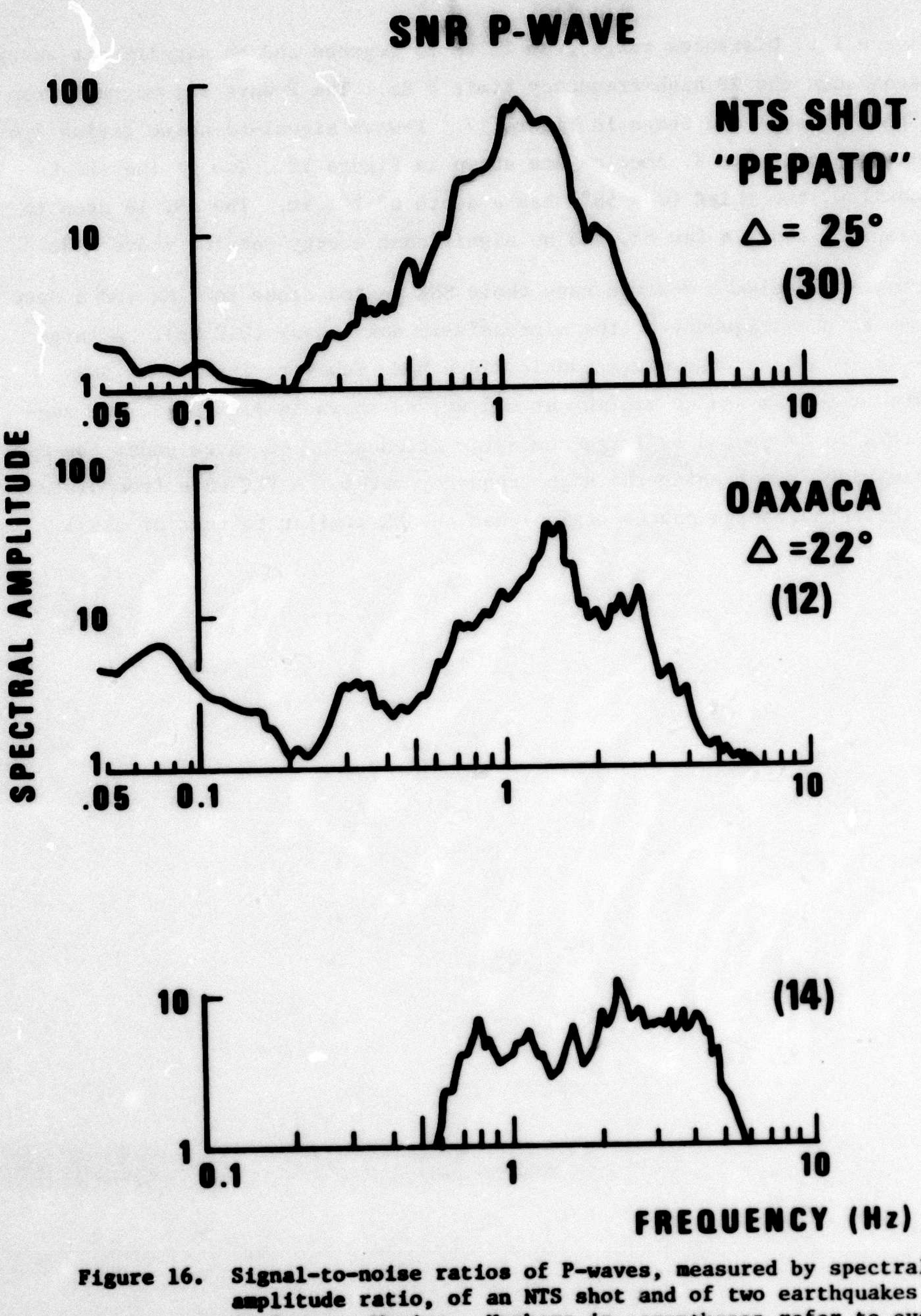

Figure 16. Signal-to-noise ratios of P-waves, measured by spectral amplitude ratio, of an NTS shot and of two earthquakes in Oaxaca, Mexico. Numbers in parentheses refer to event list in App. 1.

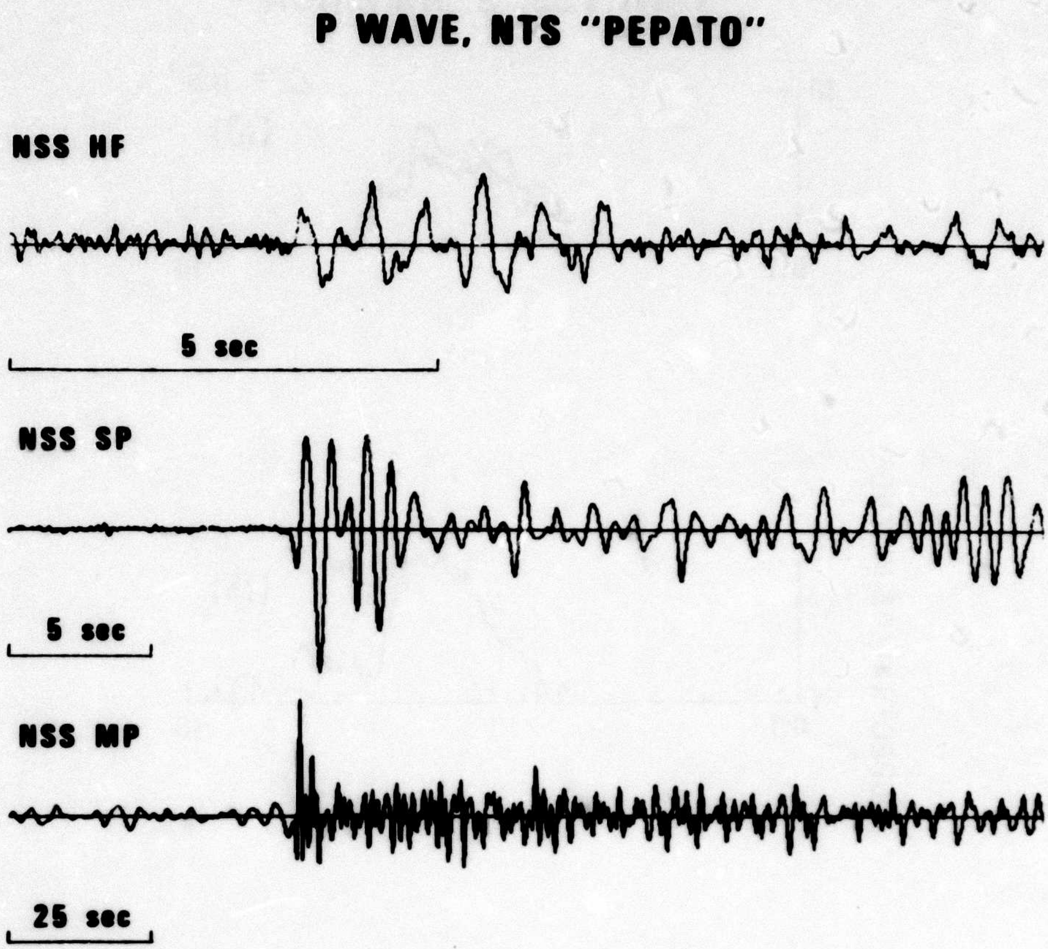

Figure 17. P-wave records on the CPO NSS HF, SP and MP channels from the underground explosion "PEPATO" at distance 25° from CPO (m_b = 5.7).

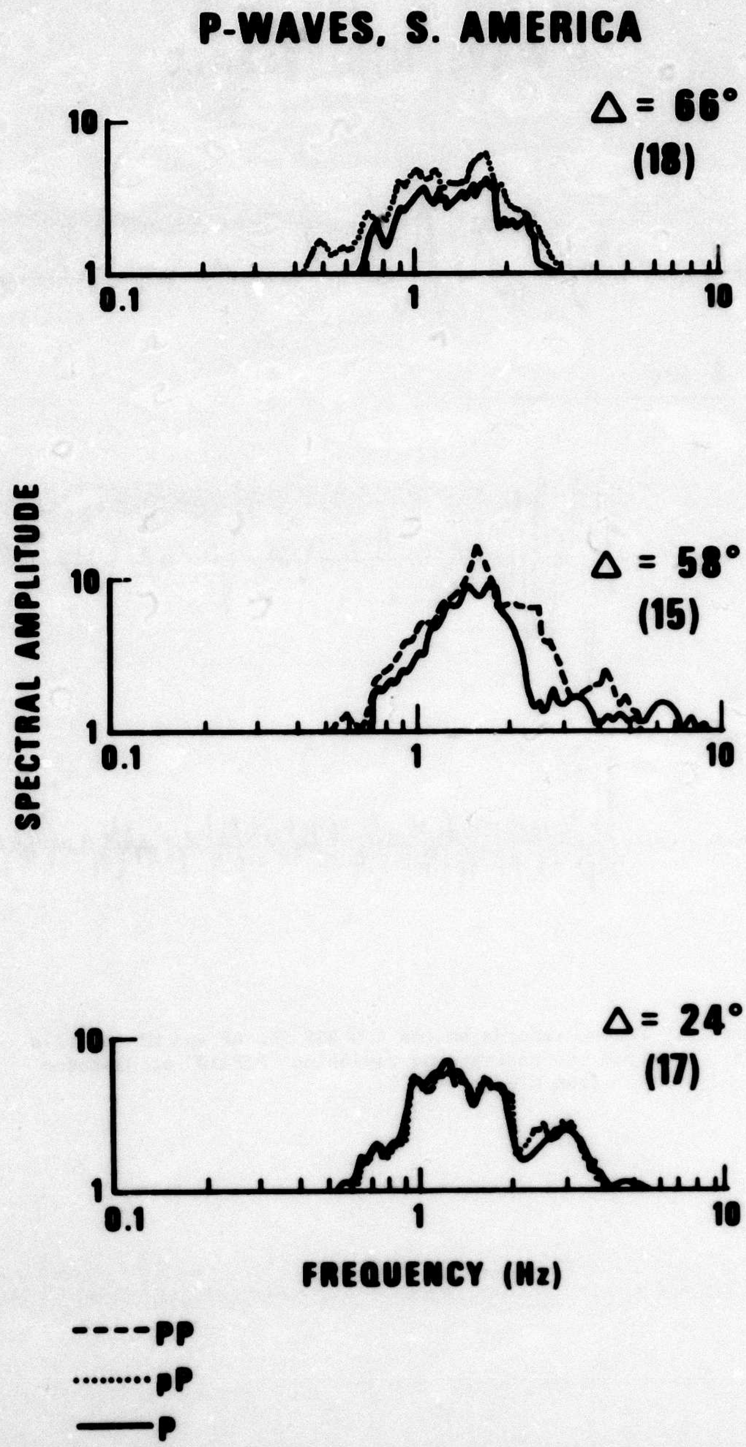

Figure 18. Signal-to-noise ratios of P-waves, measured by spectral amplitude ratio of three earthquakes in South and Central America. Numbers in parentheses refer to the list of events in App. 1.

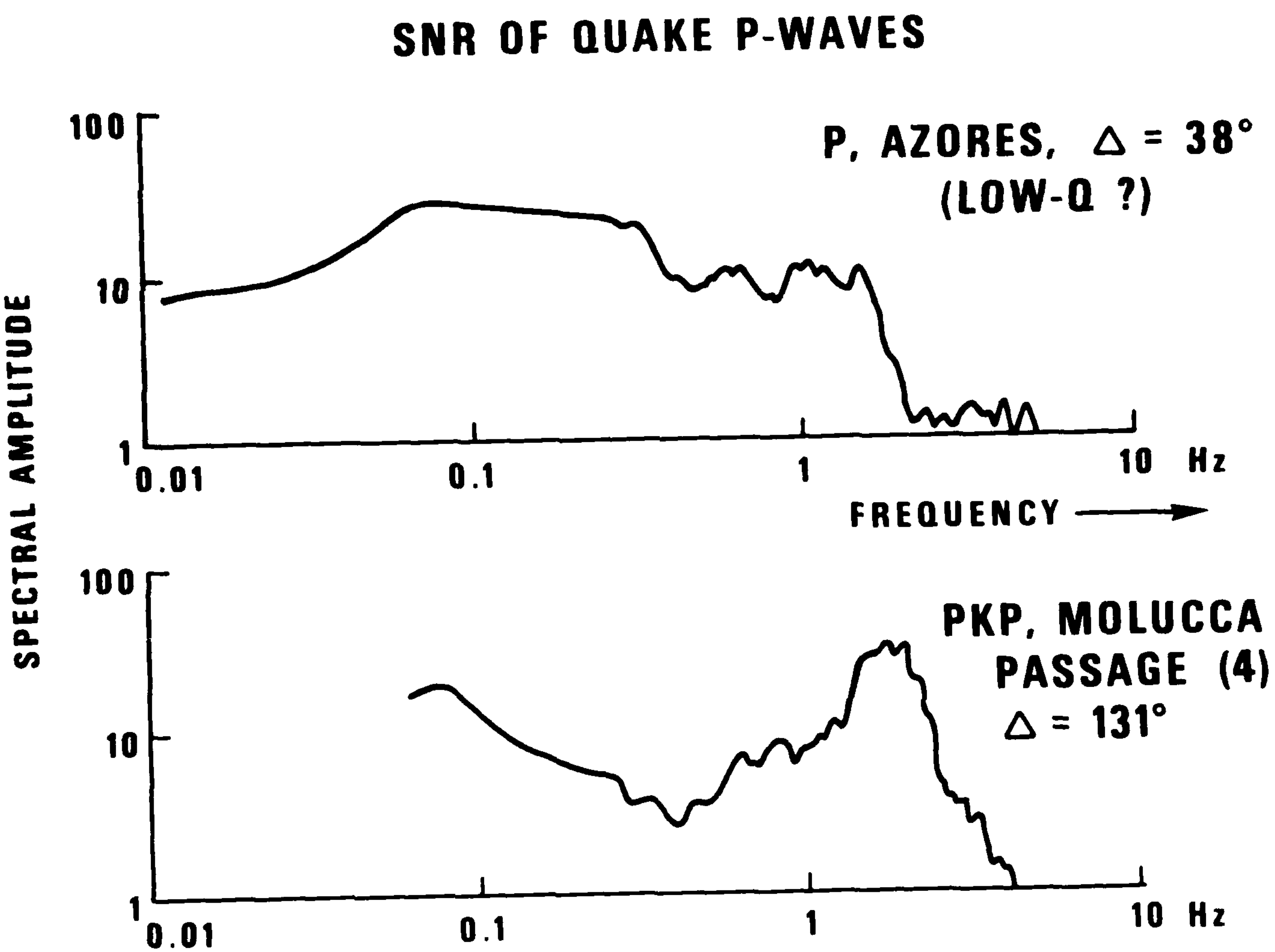

Figure 19. Signal-to-noise ratios of the P-wave from an earthquake on the Mid-Atlantic Ridge ("Azores") and of a PKP wave. The measure is the spectral amplitude ratio. Numbers in parentheses refer to the event list in App. 1.

6. RECEPTION AND PROCESSING OF NSS DATA AT THE SDAC

6.1 General

The seismological results obtained from an on-line observatory depend not only on the characteristics of the sensing instrument and A/D system, but also on all the tele-communication links and data acquisition computer systems, their processing of the data and their reliability.

On the NSS project, there were several weak areas that were uncovered as a result of implementing the on-line data acquisition that might otherwise never have been realized. Unfortunately, some of these could not be pursued as vigorously as this author would prefer. However, a large body of experience was obtained and this chapter attempts to summarize and highlight these.

This chapter is organized around the describing of the systems and their design strengths and weaknesses treated in a qualitative fashion. The emphasis of the evaluation is to address design flaws and not to test total reliability of the system. Therefore, our evaluation does not analyze "up" and "down" time intervals and their causes or similar measurements.

Based on the evaluation described in this chapter we shall recommend in our conclusions (Chapter 7) that sufficient information about the data time (to the nearest accuracy implied by the sampling rate) be transmitted to the processing center (SDAC), and that TOD, year and day-of-year, or the full WWV time code, be transmitted to the observatory, and put into the data stream. We shall suggest suitable ways of accomplishing this. We shall also recommend that the authentication scheme or suitable alternative error detector be implemented by the processing center.

6.2 Computer Configuration and Processing

6.2-1 System Design Rules

There are several important observatory site design rules that affect the NSS data processing assumptions. First, the data may possibly not be transmitted to SDAC in real-time. The data may be delayed en route. However, commands and time will be transmitted to the site in real-time.

Second, the observatory may possibly not be within range for receiving WWV data directly.

Third, the observatory must be able to operate on very low power and, therefore, may not be able to perform some functions that conceptually belong at the observatory.

6.2-2 Computer System

The diagram in Figure 20 illustrates relevant portions of the SDAC computer complement.

The tie-in to the modem is made by a microcomputer-based communications handler entitled Regional Station Interface (RSI), which conforms the experimental data to the SDAC format. Proper time information and format are essential to the SDAC where real-time seismic data is routinely collected and analyzed from observatories in the United States and Norway.

The RSI consists of several submodules, each performing one or more of the data handling functions. The unit:

-- Separates redundant data streams and synchronizes on a 32-bit code;
-- Formulates a GMT time code;
-- Converts the incoming gain-ranged format to the SDAC data format;
-- Transfers both converted and unconverted data to the Communications Control Processor (CCP) of the SDAC.

At the CCP the data enters the routine analysis and data storage system of the SDAC.

The RSI is built around a Z-80 microcomputer with MULTIBUS* external bus format and card cage. An 8-slot chassis contains 2 custom circuit boards and an off-the-shelf Z-80 single board computer with 4K ROM, 8K RAM and 2 parallel I/O ports.

The functions of the first custom board are to receive data from the modem, to separate the two bit-interleaved data streams, to perform synchronization using a 32-bit code on each one-second data block, and to transfer the two separated data streams to the second custom board.

The second custom board has an Intel 8085 microprocessor and, for its data buffer, a 4K dual-port RAM memory. After data from the first board is read into the memory and identification of the two data streams is made, a one-second data block is reorganized for processing. A control signal then is sent to the Z-80 single board computer where final formatting is

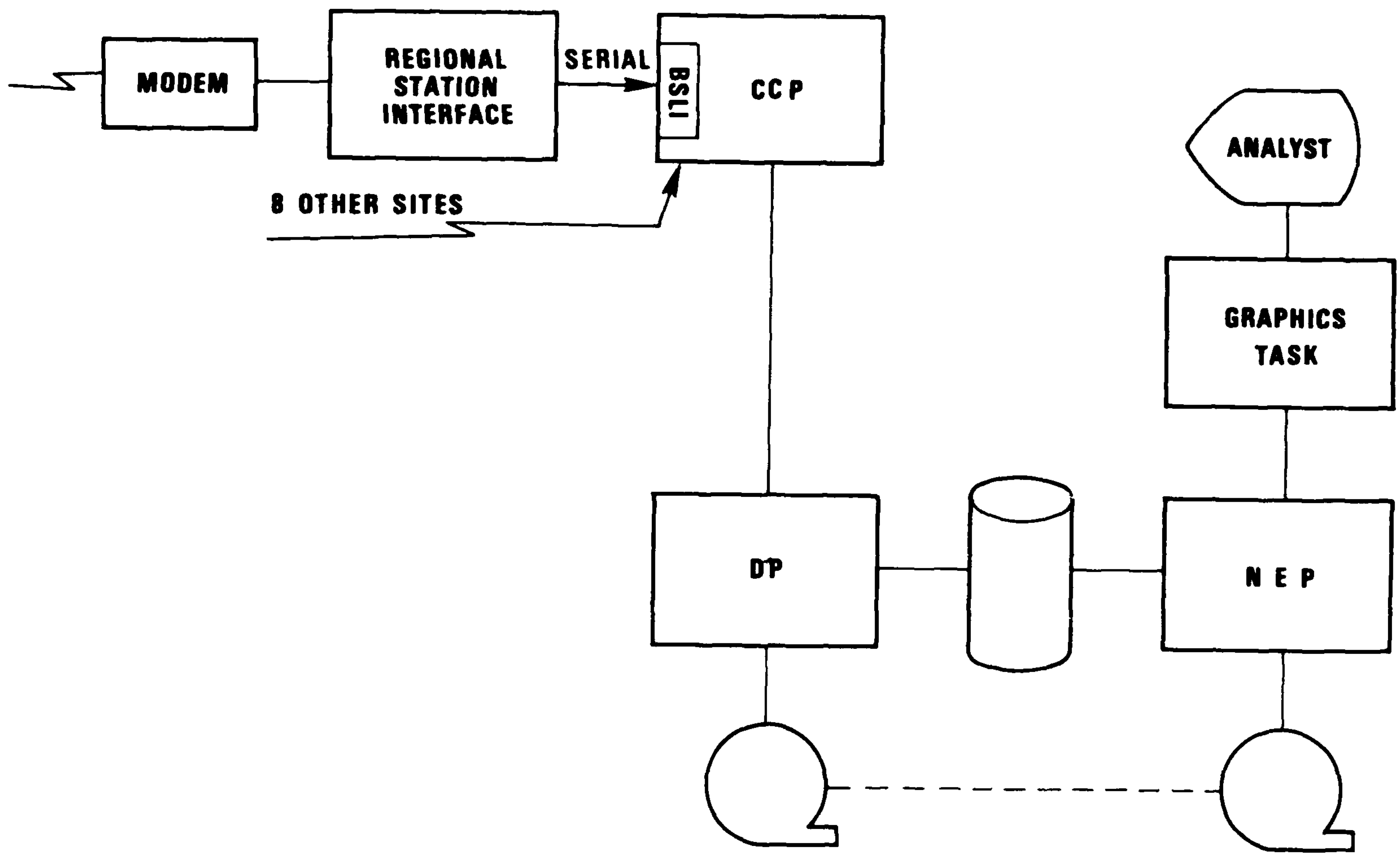

Figure 20. The computer configuration.

performed in the dual-port memory before data is transferred to the real-time computer.

6.2-3 Data Organization and Redundance Scheme

The data stream contains:

1. time information in several fields;
2. seismic data;
3. several status fields;
4. an error detection field called authentication code.

As part of the error detection and recovery scheme, there are two data streams transmitted: one in real-time and one delayed, but both are transmitted at the real-time rate. The real-time and delayed data streams are independent, but bit-interleaved. The delayed data stream is bit-inverted to distinguish it from the real-time data. The initial implementation of the NSS site at SDAC merely separates the two streams, and processes the real-time data stream. No processing takes place on the delayed data. No error detection is done using the authentication code.

Reference observatory design rules; though the entire stream might have been shifted in time (delayed) for this project it did not appear to be delayed at all.

6.2-4 Computer Processing, The Original Design Objectives

The original design rules for the implementation at the SDAC were:

1. The impact of integrating the NSS data into the normal operation of the SDAC is to be minimized.

2. The design is to facilitate a phased implementation. We planned to implement only the critical features first and add additional features later.

3. Hardware developed for the system should be easily changed to perform different functions that may be dictated by future versions of the system.

4. Reliability should be at least as good a level as the other on-line data at the SDAC.

* MULTIBUS is a trademark of Intel Corporation.

6.2-5 Processing in the Regional Station Interface

To meet the first objective requires that the NSS data be presented to the CCP and in turn to the other systems in a form that most nearly matches that of the other on-line observatory sites. Therefore, the RSI is assigned the tasks (1) to reform the data words to one of two SDAC formats, (2) to reorganize block format to SDAC block format and (3) to construct a full time code corresponding to the first data sample of the 1-second block.

To meet the normal SDAC error detection level, the RSI forms a VELANET message for transfer to the CCP. The VELANET messages contain a check sum error detection feature. However, this feature only validates the transfer from the RSI to the CCP.

Word Conversion. The 20-Hz data, which is used for on-line detection, is converted to 16-bit integer form. When the sample value exceeds a 16-bit field, the highest positive or negative value is substituted.

All other data is converted to the gain-range format. In this case, precision is sacrificed in certain ranges. There are 4 bits for gain-code and 12 bits of signed mantissa.

In addition to the converted data, a copy of the data in the original word format is retained such that each one-second block of data contains two copies of the entire sample complement.

Time Word Construction. The time information in the data transmission block consists of several fields. This information together with the year, day-of-year from local SDAC sources are used to contruct the data time. The time information in the data block is shown in Figure 21.

The RSI uses bits 2^{23} through 2^{0} from TIME1 and bits 2^{27} through bits 2^{24} from TIME2 to make up a message count. Bit $2^{\emptyset}$ is incremented at about the mid-point of the data sampling interval contained in a message block. Minutes, seconds and milliseconds are read from the COMMAND field adjusted by 1.5 second--the estimate of the delay between the transmission of the WWV time from the terrestrial station and the receipt and retransmission from the site. The Julian day, and hours are read from the local TOD. The

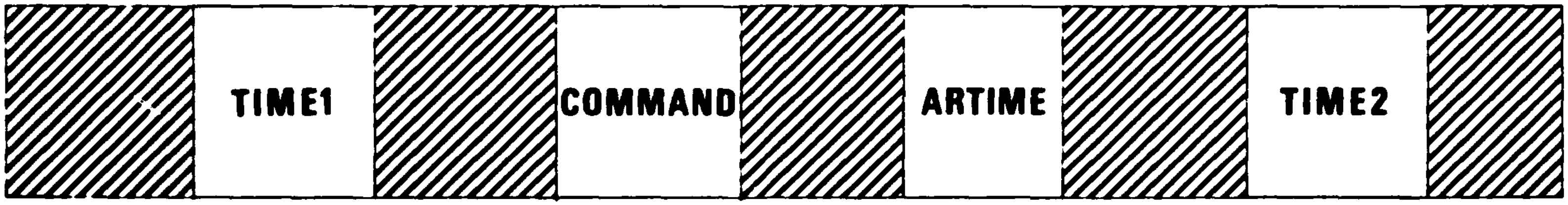

TIME1	A 24-bit binary frame counter. These 24 bits represent bits 2^{23} through 2^0 of the internal time keeping register with bit 2^0 toggling every second. The 24 bits alone are transmitted least significant bit first.
COMMAND	A 32-bit pattern indicating the last command received from the terrestrial station. This pattern is used for command verification. When no other command is being transmitted, the time command is transmitted. The time consists of minutes, seconds, and milliseconds of WWV at the terrestrial station. When no command is transmitted this field contains its previous contents. This condition can occur when the transmission link to the observatory is inoperative.
TIME2	A 24-bit binary frame counter that is mostly redundant to TIME1. These 24 bits represent bits 2^{27} through 2^{24} and bits 2^{19} through 2^0 of the internal time keeping register with bit 2^0 toggling every second. Bits 2^{27} through 2^{20}, which are taken from TIME1 and TIME2, uniquely determine which authentication variable is being used to authenticate the present frame.
ARTIME	Arrival time. A 16-bit number that indicates the arrival time of the last received command, with a resolution of about 1 msec. These 16 bits represent bits 2^5 through 2^{-10} of the internal time keeping register with bit 2^0 toggling every second.

Figure 21. The time information in the data transmission block.

year is a constant to be read from a thumb-wheel switch on the front panel since the year is not available on the local TOD. From this information, with appropriate adjustments, the time code is constructed.

When the COMMAND does not contain the time, the RSI takes the difference between the current TIME and the previous TIME1 and adds this increment to the previous complete time. Any actual time-of-day information depends on the COMMAND link of the terrestrial station to the site as illustrated in Figure 22.

6.2-6 Processing the CCP and DP

The CCP does error detection using the VELANET checksum and sets the usual communication status flags. The normal facility to display the incoming data on the CRT is available as well as all the periodic logging of status information.

In the DP system detection processing is done as well as data recording. Data is available to and processed by the NEP in the usual fashion.

6.3 Performance and Major Deficiencies

6.3-1 Performance

As stated above, this section does not attempt to give a full system performance, but a few qualitative statements do bear on the seismological results.

The first implementation of the RSI did not construct the time code. Instead, the time that the data was received by CCP was placed on each data block by the CCP. This practice was followed for most of the evaluation period because of time code problems in the data and other project delays. The time was, therefore, in error by at least 1.5 seconds for much of this period.

Data Polarity. During the course of the evaluation period there were a couple of points in time when the data polarity changed, i.e., each bit in the data stream was inverted. Since data inversion is the means by which the real-time data is distinguished from delayed data, these inversions had the effect of the data time suddenly differing from time code by about 15 minutes. The CCP passed the data onto the DP system this way.

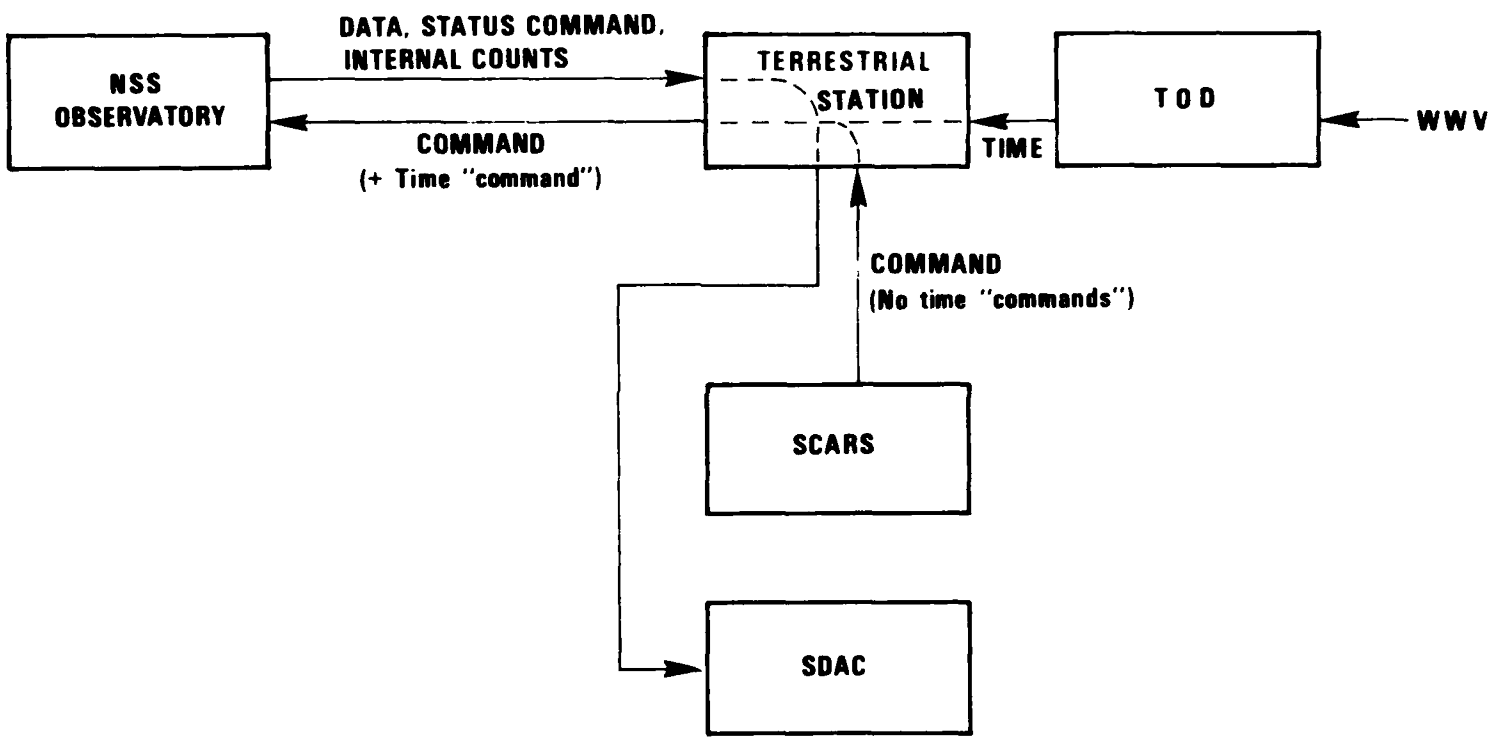

Figure 22. Flow of time information in the NSS-SDAC data transmission.

Another important computer processing factor affecting the seismological results is that the data sample word polarity was found, with assistance and concurrence by the observatory contractor, to be opposite from what was originally documented. Negative numbers indicated positive earth motion and vice versa. The RSI never changed the sign of the data words though the RSI would do so in future implementations.

6.3-2 Major Deficiencies

Error Detection. The error detection scheme was not implemented in the initial version of the RSI. There is an authentication code which is computed by the site and placed in the transmitted data. The authentication code is computed again at the receiving site and then the two authentication codes are compared. If there is a discrepancy, then the data is assumed to be bad.

One of the problems encountered in trying to construct time word is that the time code received in the data stream was sometimes invalid perhaps due to transmission errors, but since there was no error detection, the system was vulnerable to this kind of problem.

Time Error Reporting. Some information as to the fact that the terrestial station is transmitting its own local time code and the estimate of the time error is not included in the data record. The time code is transmitted from the terrestrial station over satellite link to the site and then in turn is transmitted back in a COMMAND field in the data block. When the terrestrial station is not receiving WWV because of radio interference, it sends clock time to the site; however, this time can have a progressively enlarging error.

Year Handling. The type of algorithm needed to compute the time-of-day makes it particularly difficult to deal with the year roll-over.

7. CONCLUSIONS AND RECOMMENDATIONS FOR FUTURE VERSIONS OF THE DATA TRANSMISSION SYSTEM

Seismological Conclusions

Seismometers in the prototype NSS system and those from an SDCS station were installed at a common depth of 100 meters in two boreholes separated by 10m at CPO to compare their outputs in several ways. First, we wanted to test the precision and clipping level of gain ranging in the analog-to-digital conversion subsystem of the NSS. We also wanted to study signal-to-noise ratios of local, regional, and teleseismic events in the broad frequency range covered by the four channels of the NSS.

The large dynamic range of the NSS system makes clipping a rare phenomenon, though it was observed. When clipping did occur, teleseismic events clipped first on the LP channel and then on the MP channel. We observed that events clipped by the LP system can be recovered from the unclipped MP channel with suitable filtering. We also found that clipping on the MP channel could be expected from distances of 30 degrees or less when the event magnitude (M_s) was 7.0 or larger. Regional events clipped first on the SP channel, when epicentral distance was 5 degrees or less and the event magnitude (m_b) was larger than 5.5.

Non-linear effects may occur when large, high-frequency oscillations arrive at the seismometer and cause spurious pulses to appear on the LP and MP channels.

The resolution in describing the Earth noise waveform is good; the rounding error is from 0.1% to 0.3% of the RMS noise amplitude under low noise conditions, such as those normally prevailing at night time.

The NSS and SDCS sensors give similar noise and signal spectra when the instrument responses are considered, except near the folding frequency where the strong anti-aliasing filters in the NSS system reduce signal power. Coherences computed for four separate time periods in the NSS system (night-time noise) indicate that the earth-to-system noise ratios are good for frequencies up to 60% of the folding frequency; two exceptions to this were the vertical SP channels where 6 Hz is the upper limit for energy definition. In the first case, a very sharp drop in the earth signal-to-system noise ratio began in some cases at 4 Hz. In the second case, the HF channel sometimes had poor signal fidelity near 2 Hz (when recording night-time earth noise). Generally, the design goal of being able to record the Earth noise up to 50%

of the folding frequency was fulfilled.

When recording regional events at distances less than 5 degrees, a sampling rate of 60 samples-per-second seems justified, because signal-to-noise ratios were large for various seismic phases propagating at frequencies up to 20 Hz. If we assume a Q value of 1000 for L_g waves, as Hermann (1980) does, the loss in signal amplitude when the waves propagate from 5 to 10 degrees would be 10 times larger for waves at 10 Hz than for waves at 5 Hz. We conclude that energy above 6 Hz, which is the practical upper limit for data sampled at 20 times-per-second, is important to the location and analysis of events recorded at distances up to 5 degrees, and is less important in the analysis of events recorded beyond 5 degrees.

Recommendations for Future Versions of the System

The following list gives our recommendations for future versions of the transmission and reception system:

1. Since seismological analysis depends on accurate time, we recommend that sufficient information about the data time be transmitted to the (SDAC) to make the time determination as precise as the sampling rate.

2. We recommend that a TOD, year, and day-of-year be transmitted to the observatory and that complete time code be put into the data stream, thus eliminating dependence on a second transmission leg to provide accurate timing. The Navy's orbiting satellite TRANSIT might be used for TOD, in conjunction with a receiver and local low-drift TOD for a sustained time read out at the observatory.

3. An alternative approach is to have the control link transmit the full WWV time code, when available. When WWV is not available, the observatory would transmit the last good time code, the time interval since the last good WWV time, and the error estimate for the time interval.

4. As a minimum, we recommend that the terrestrial station transmit to the observatory the full WWV when available. When the terrestrial station must use its local clock because WWV is not being received, we recommend that this fact be indicated in the data stream to the processing center (SDAC) and that the time error estimate be added to the data stream.

5. We recommend that the authentication scheme or a suitable alternative error detector be implemented by the processing center.

6. The data format should conform to the practices of the seismological community.

7. Attempts should be made to digitize on an even-second boundary.

8. We suggest that sufficient buffer space be allocated to reconstruct a single data stream from the delayed and real-time data. This should be done prior to detection processing.

9. We also recommend that sufficient buffer space be allocated to time align other data sources with the NSS data.

10. Current NEP maintains time to the nearest decisecond. We recommend reformatting this value to accommodate varying sample rates.

ACKNOWLEDGEMENT

The authors thank Dr. Shumway for helpful discussions in application of computations of coherence.

REFERENCES

Durham, H. B. (L979). NSS seismic data system, design goals and rationale; manuscript (Sandia Laboratory), February 14.

Fitch, T. S. and M. W. Shields (1979). Amplitude spectra of crustal phases from a Canadian earthquake, Semiannual Technical Summary (Seismic Discrimination) Lincoln Laboratory, 31 March.

Goncz, J. and I. Noponen (1979). Relationship between M_s and m_b for small earthquakes in Uzbekistan, USSR, VELA Seismological Center Research Review, 26-27 September.

Herrmann, R. B. (1980). Q estimates using the coda of local earthquakes, Bull. Seism. Soc. Am., 70, 447-468.

Otnes, R. K. and L. Enochson (1978). Applied Times Series Analysis, Volume I., Basic Techniques, John Wiley and Sons, New York.

Romney, C., B. G. Brooks, R. H. Mansfield, D. S. Carder, J. N. Jordan and D. W. Gordon (1962). Travel times and amplitudes of principal body phases recorded from GNOME, Bull. Seism. Soc. Am., 52, 1057-1074.

von Seggern, David (1977). Amplitude distance relation for 20-second Rayleigh waves, Bull. Seism. Soc. Am., 67, 405-411.

APPENDIX I

THE DATA USED IN THIS STUDY

Appendix I

The Data Used in This Study.

(1) EVENTS

Event Code	Distance to CPO	m_b	M_s	Region	Depth	Date	GMT Time
(a) Teleseismic Events ($\Delta > 20°$)							
4	131°	6.3	6.9	MOLUCCA PASSAGE	20	4-10	1-42-21
9		4.6		N. ATL. RIDGE	33	4-10	10-33-00
10	38°	5.5	5.9	N. ATL. RIDGE	33	4-22	9-50-18
12	22°	4.9		OAXACA (MEX.)	0	4-02	3-46-04
14	21°	4.4		OAXACA (MEX.)	29	5-30	8-4-21
15	58°	5.1		N. CHILE	101	4-21	22-16-25
16	62°	4.3		ARGENTINA	202	4-20	23-25-13
17	24°	4.1		NICARAGUA	30	4-24	11-13-01
18	66°	-		CHILE-ARGENTINA	117	4-11	1-44-02
30	25°	5.7		NTS SHOT "PEPATO"		6-11	14-00-00
-			7.6	MEXICO		3-14	
(b) Regional Events							
2	4.6°					4-09	21-32-43
6	3.2°	2.8		S. CAROLINA	5	5-04	12-13-04
19	4.0°	3.0		ARKANSAS	9	6-25	17-11-14
31	1.0°	3.6		TENNESSEE	8	8-31	5-18-57
32	3.5°	2.7		MISSOURI	2	7-13	7-29-39
(c) Local Events ($\Delta < 1°$)							
1	21 km					4-10	22-31
5	21 km					4-09	21-30

(2) NOISE SAMPLES

Code	Date	Time (Local)
1	4-10	05-10 P.M.
22	4-10	08-08 P.M.
23	4-10	11-02 P.M.
24	4-10	02-30 A.M.
25	4-10	12-00 P.M.
26	5-03	22-32 P.M.
27	5-03	01-30 A.M.
28	4-20	01-30 A.M.
29	4-20	07-24 A.M.